

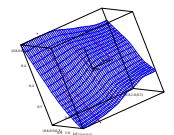
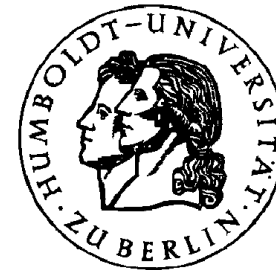
# Voles, Volas, Values

Matthias R. Fengler

Wolfgang K. Härdle

Institut für Statistik und Ökonometrie  
Humboldt-Universität zu Berlin

Center for Applied Statistics and Economics  
(CASE)



# Microtus Ochrogaster

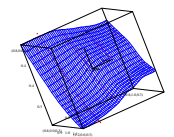
---

Prairie Vole

Order Rodentia (Nager): Family Muridae (echte Mäuse) : *Microtus Ochrogaster*

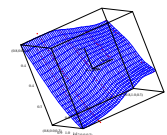


Figure 1: *Microtus Ochrogaster*



## Description & habits:

- dark brownish or blackish mouse; total length 146 mm, tail 34 mm on average
- inhabits Hardin County in southeastern Texas, and in the extreme northern Panhandle.
- lives in tall-grass prairies in colonies, utilizing underground burrows and surface runways under lodged vegetation for concealment
- food almost entirely vegetable including green parts of plants, seeds, bulbs, and bark, much of which they store for winter use



# Microtus Californicus

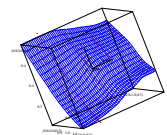
---

California Vole

Order Rodentia (Nager): Family Muridae (echte Mäuse): *Microtus Californicus*

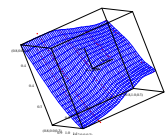


Figure 2: *Microtus Californicus*



## Description & habits:

- grizzled brownish mouse, gray below; total length, 157-214 mm; tail, 39-68 mm
- known in Southwestern Oregon through much of California
- inhabits grassy meadows from sea level to mountains
- is a burrower, but it also forms surface runways
- food is almost entirely vegetable including green parts of plants, seeds, bulbs, and bark



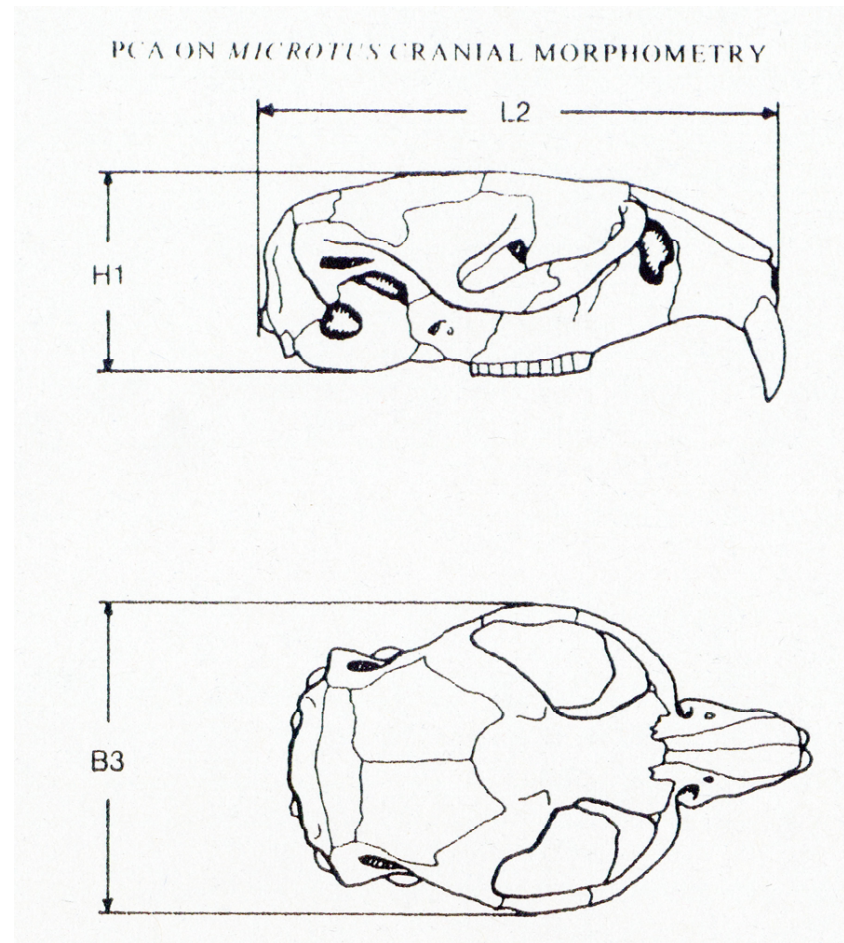
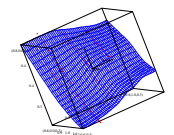


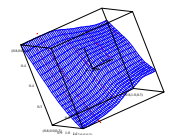
Figure 3: *Diagram of cranial measurements; L2 condylo-incisive length, B3: zygomatic width, H1: skull height. Taken from Aioldi and Flury (1988).*



# Common Principle Components

Common principle components has been used for morphometric purposes to estimate a joint eigenstructure for the cranial measurements of voles, Airoidi and Flury (1988).

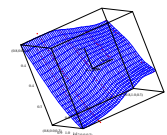
This data contains cranial measurements for four natural groups of the animals: two sexes in two species. The measurements include the condylo-incisive length (L2), the zygomatic width (B3) and the skull height (H1) (Figure 3).



# Key Hypothesis of CPC

Impose

- a joint eigenstructure  $\Gamma$  on population covariance matrices  $S_i$ ,
- while in-group variances (= eigenvalues  $\lambda_i$ ) are not restricted.





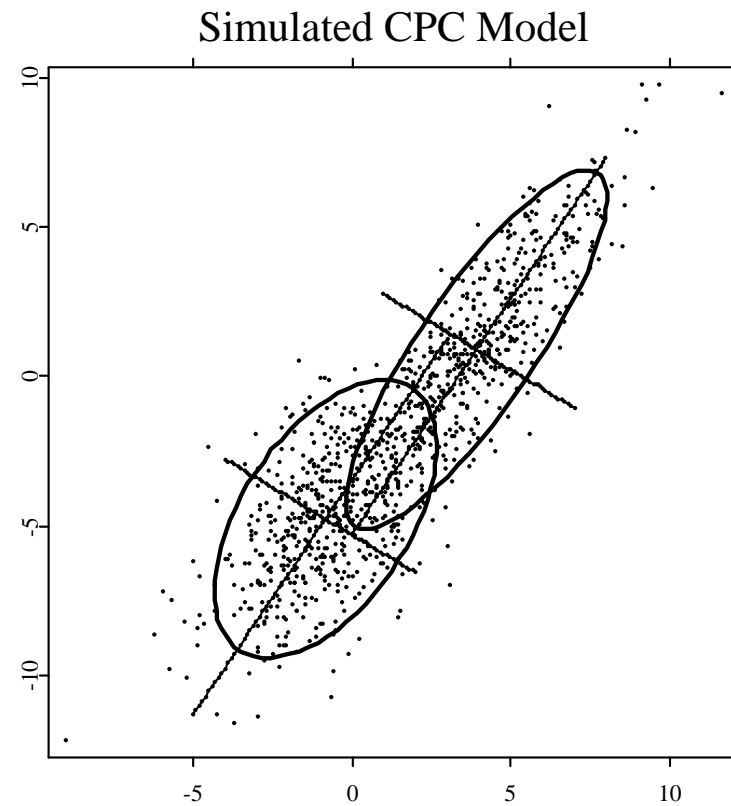
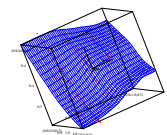


Figure 4: *Simulated CPC model as observable in vole data; compare Airoidi and Flury (1988)*

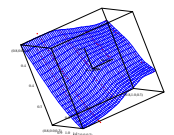


## Voles: What did we learn?

### CPC

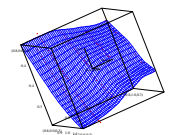
- allows for estimating a common eigenstructure in the presence of different group variances.
- helps identify morphometric structures across different species and sexes.

Using a simple PCA instead in grouped data may lead to biased estimates.



# Overview

1. **Voles**: Zoological Motivation ✓
2. **Volas**: Implied Volatility Surface Dynamics
3. Principal Components Analysis
4. *Common* Principal Components Analysis
5. Estimation, Selection, Prediction
6. **Values**: Trading Strategies, Risk Management

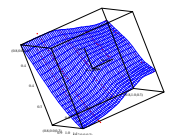


## Implied Volatility Surface Dynamics

# The Black-Scholes Model, Implied Volatilities and the Smile

Based on the assumption that asset prices follow a geometric Brownian motion, the Black and Scholes (BS) formula values European options:

$$C_t^{BS} = S_t \Phi(d_1) - K e^{-r\tau} \Phi(d_2)$$

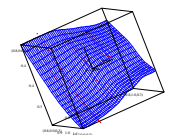


# BS Formula

$$C_t^{BS} = S_t \Phi(d_1) - K e^{-r\tau} \Phi(d_2)$$

$$d_1 = \frac{\ln(S_t/K) + (r + \frac{1}{2}\sigma^2)\tau}{\sigma\sqrt{\tau}} \quad d_2 = d_1 - \sigma\sqrt{\tau}$$

$\Phi$	CDF of the standard normal distribution	$r$	Interest rate
$S_t$	Asset price	$\tau = T - t$	Time to maturity
$K$	Strike price	$\sigma$	Constant volatility parameter

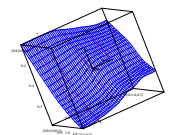


## BS Formula

Suppose  $S_t = 230$ ,  $K = 210$ ,  $r = 5\%$ ,  $\tau = 0.5$ , and  $\sigma = 25\%$ .  
Then the call price is given by  $C_t^{BS} = 30.98$  and the put price  
 $P_t^{BS} = 5.92$ .

You can derive the  $P_t^{BS}$  also by the put-call-parity:

$$\begin{aligned} C_t - P_t &= S_t - Ke^{-r\tau} \\ 30.98 - 5.92 &= 230 - 210e^{(-0.05 \cdot 0.5)} \end{aligned}$$

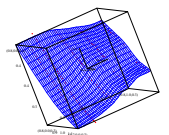


# Implied Volatilities

However,  $\sigma$  is unknown! Hence define the volatility  $\hat{\sigma}$  *implied* by observed market prices  $\tilde{C}_t$  as

$$\hat{\sigma} : \quad \tilde{C}_t - C_t^{BS}(S_t, K, \tau, r, \hat{\sigma}) = 0$$

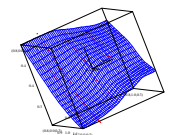
This solution may be found by using a Newton-Raphson or a bisection algorithm. It is unique as the BS formula is globally concave in  $\sigma$ .



# Implied Volatilities

## Empirical Findings

- Implied volatility is not constant across time  $t$ .
- Implied volatility is not flat across strikes.
- Implied volatility is not flat across time to maturity.
- Implied volatility became asymmetric since the 1987 stock market crash.





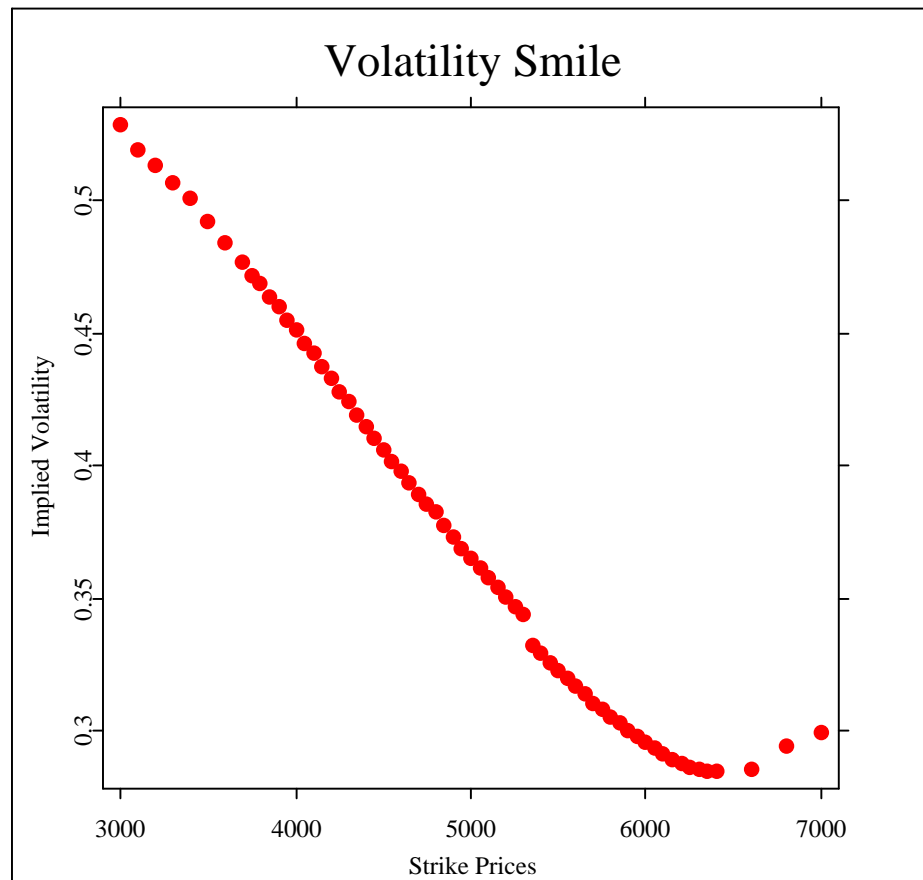
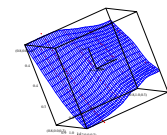


Figure 5: *Vola smile/smirk: 3 months to expiry,  $t = 990104$ , ODAX*



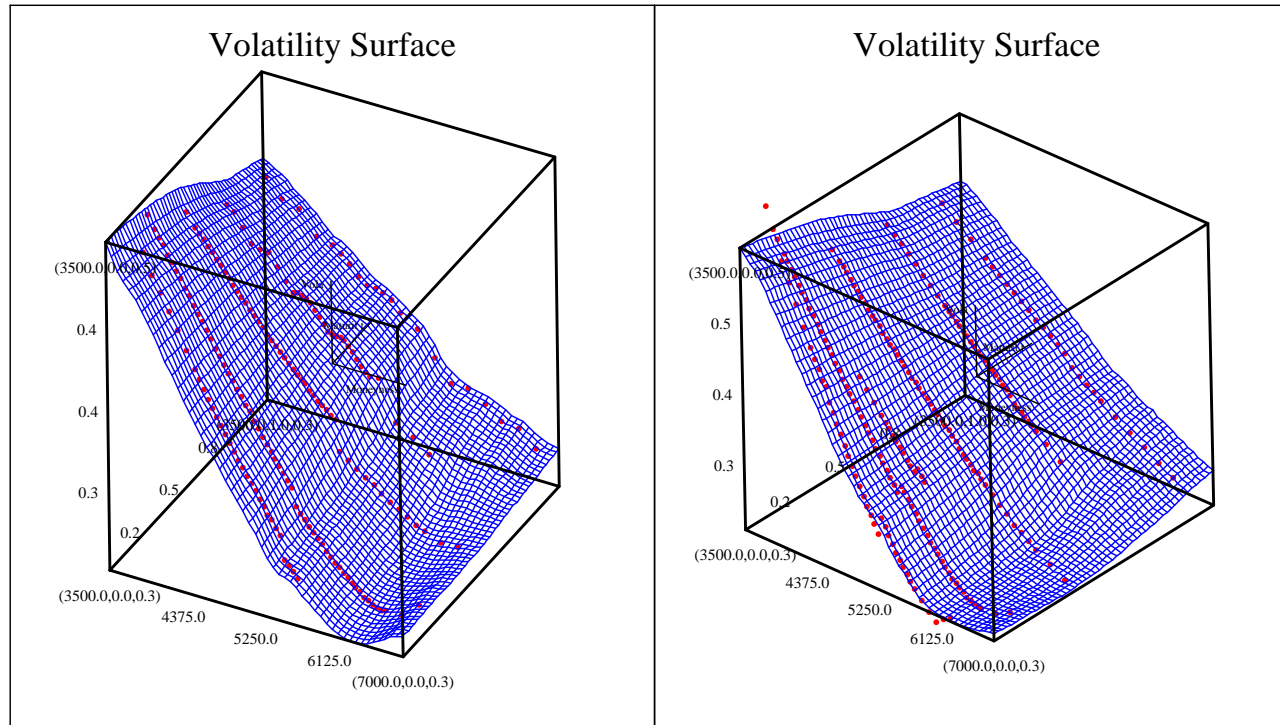
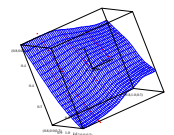


Figure 6: *Implied Volatility Surfaces:  $t_1 = 990104$  and  $t_2 = 990201$ , ODAX*

 [CPCdoubleSurf.xpl](#)



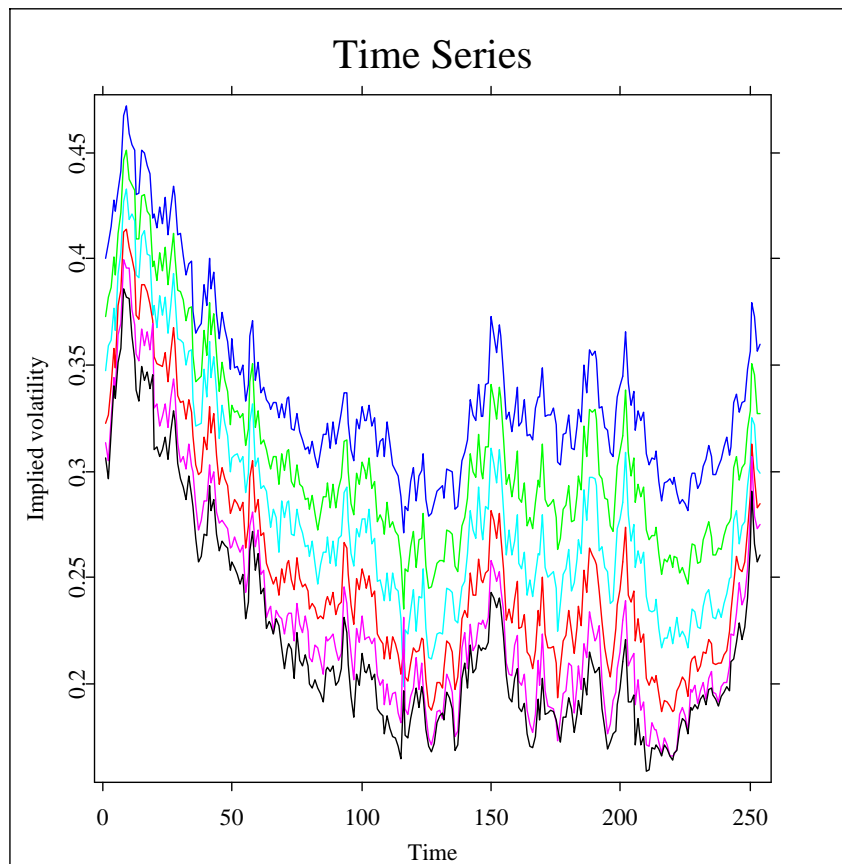
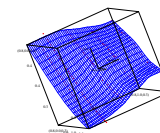


Figure 7: *Time series 1999 of implied volatilities across the smile: 3 months maturity*  
–  $\kappa = 1.10$  up to  $\kappa = 0.85$ , ODAX



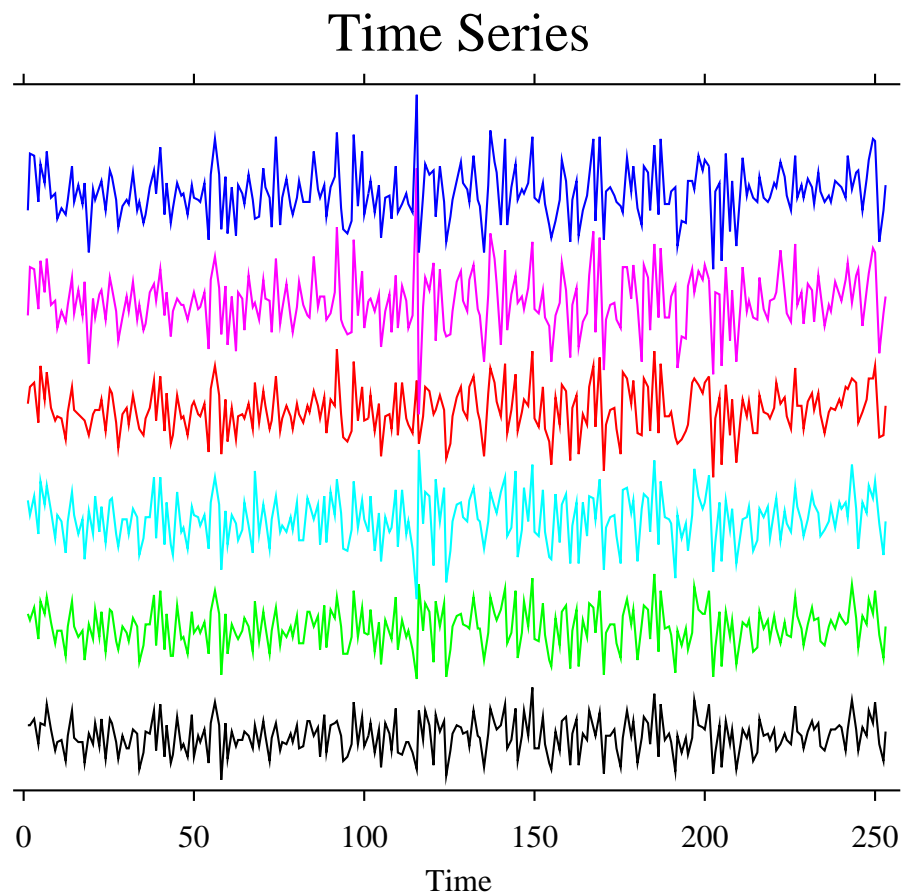
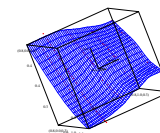


Figure 8: *Time series 1999 of log-returns of implied volatilities across the smile: 3 months maturity –  $\kappa = 1.10$  up to  $\kappa = 0.85$ , ODAX*



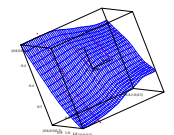
# Importance of Implied Volatilities

## Practitioners' point of view

- BS-formula serves as a convenient mapping from the spaces of prices, maturities, interest rate, strikes to the real line
- Trading rules can be based on implied volatilities
- Volatility contracts (e.g. VDAX) are based on implied volatilities

## Theoretical point of view

- Pricing of illiquid or exotic options by directly modeling implied volatilities: Market Models of Volatility (Dupire, 1994, Derman and Kani, 1989, Schönbucher, 1999)



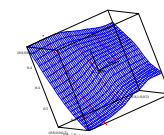
# Purpose of the study

Understand the dynamics of implied volatilities:

- identify the number and shape of shocks driving the surface
- reduce the dimension of the surface vector time series

## Plan

- Estimate **nonparametrically** the implied volatility surface  $\hat{\sigma}_t(\kappa, \tau)$  on a fixed grid of moneyness  $\kappa_i = \frac{K}{F_{\tau t}}$  and maturity  $\tau_j$  ( $F_{\tau t} = S_t e^{r\tau}$  is the implied future price).
- Apply **(Common)** Principle Components Analysis to  $\Delta \ln \hat{\sigma}_t$
- Study common factors and their dynamics

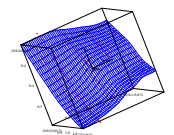


# Nonparametric Smoothing

For a partition of explanatory variables  $(x_1, x_2)^\top = (\kappa, \tau)^\top$ , i.e. of moneyness and maturities, the two-dimensional Nadaraya-Watson kernel estimator is given by

$$\hat{\sigma}_t(x_1, x_2) = \frac{\sum_{i=1}^n K_1\left(\frac{x_1 - x_{1i}}{h_1}\right) K_2\left(\frac{x_2 - x_{2i}}{h_2}\right) \hat{\sigma}_{ti}}{\sum_{i=1}^n K_1\left(\frac{x_1 - x_{1i}}{h_1}\right) K_2\left(\frac{x_2 - x_{2i}}{h_2}\right)},$$

where  $\hat{\sigma}_{ti}$  is the volatility implied by the observed option prices  $\tilde{C}_{ti}(\kappa, \tau)$  or  $\tilde{P}_{ti}(\kappa, \tau)$  respectively,  $K_1$  and  $K_2$  are univariate kernel functions, and  $h_1$  and  $h_2$  are bandwidths.



# Nonparametric Smoothing

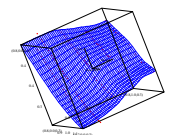
## Kernel choice

An order 2 quartic kernel:

$$K(u) = \frac{15}{16} (1 - u^2)^2 I(|u| \leq 1).$$

## Bandwidth choice

A **penalizing function technique** yields asymptotically optimal bandwidths  $h_1$  and  $h_2$  as a starting point.





# Principal Components Analysis

For illustration we pick two time series of implied volatility returns from different parts of the smile ( $\kappa = 0.90$  and  $\kappa = 1.10$ ) at a fixed one-month maturity:

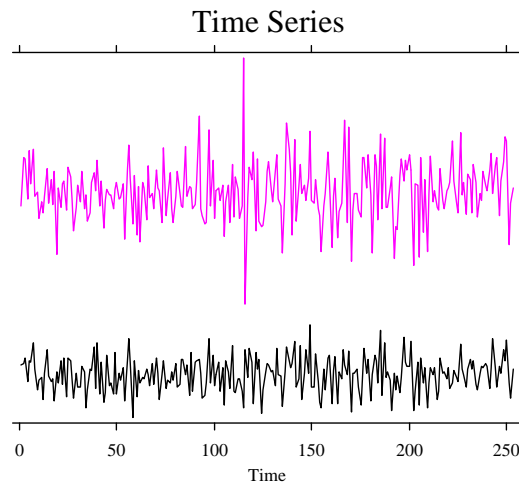
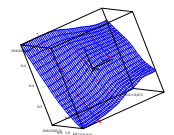


Figure 9: 1 months maturity - moneyness is  $\kappa = 0.90$  against  $\kappa = 1.10$ , ODAX



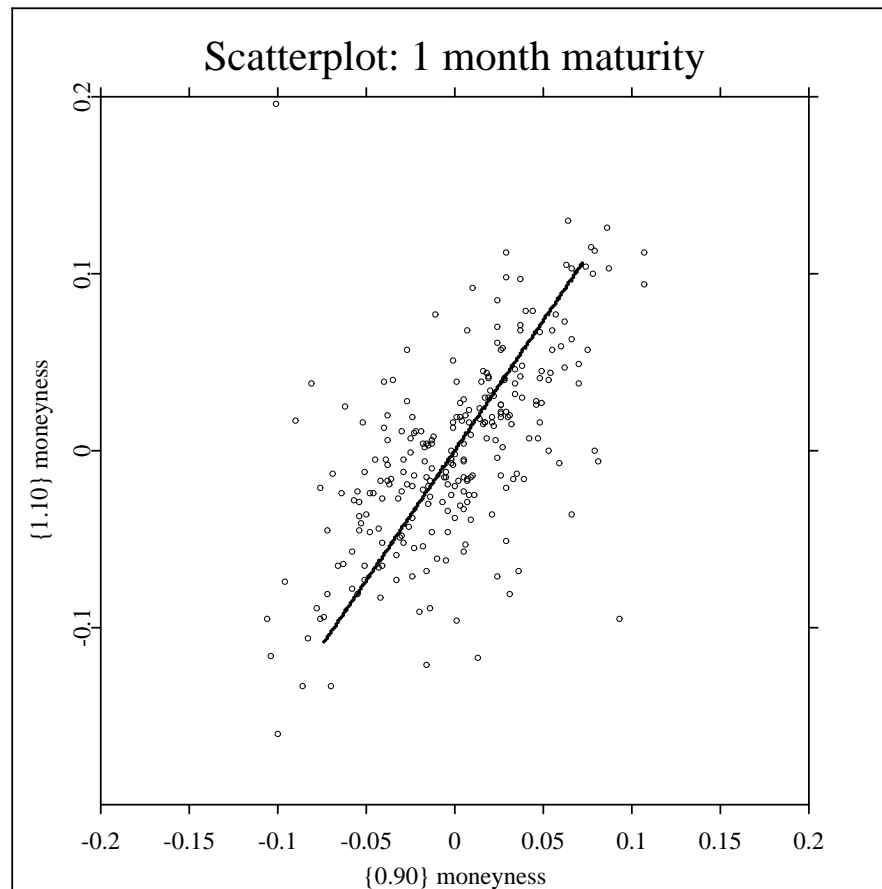
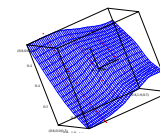


Figure 10: 1 months maturity - moneyness is  $\kappa = 0.90$  against  $\kappa = 1.10$ , ODAX



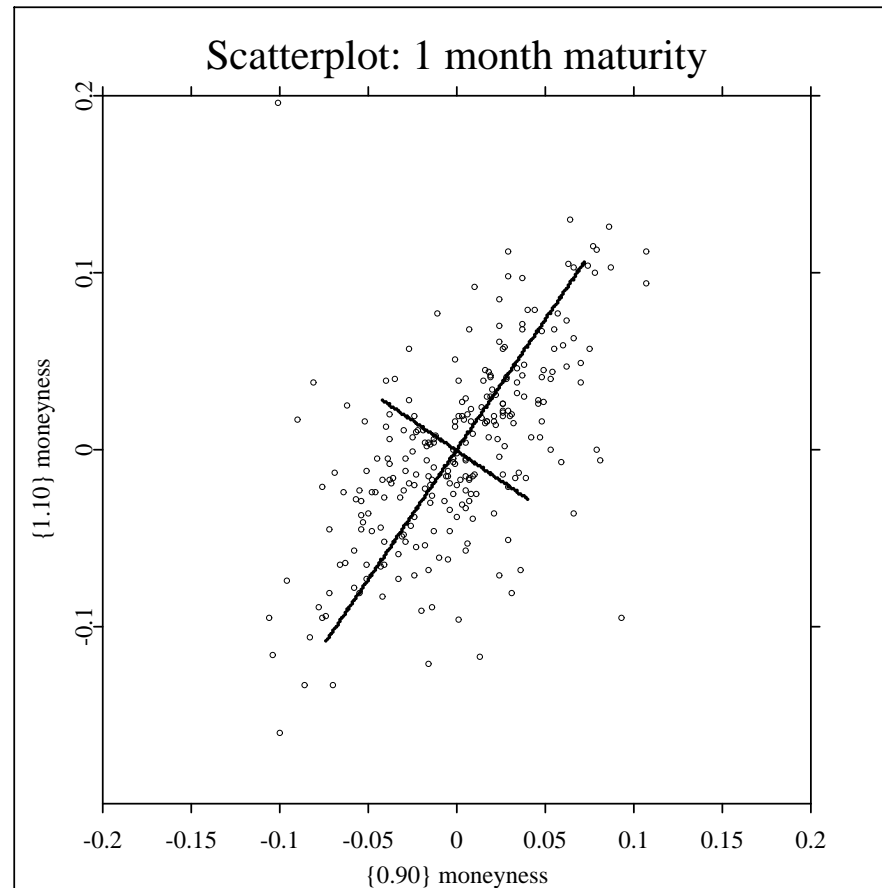
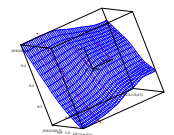


Figure 11: 1 months maturity - moneyness is  $\kappa = 0.90$  against  $\kappa = 1.10$ , ODAX



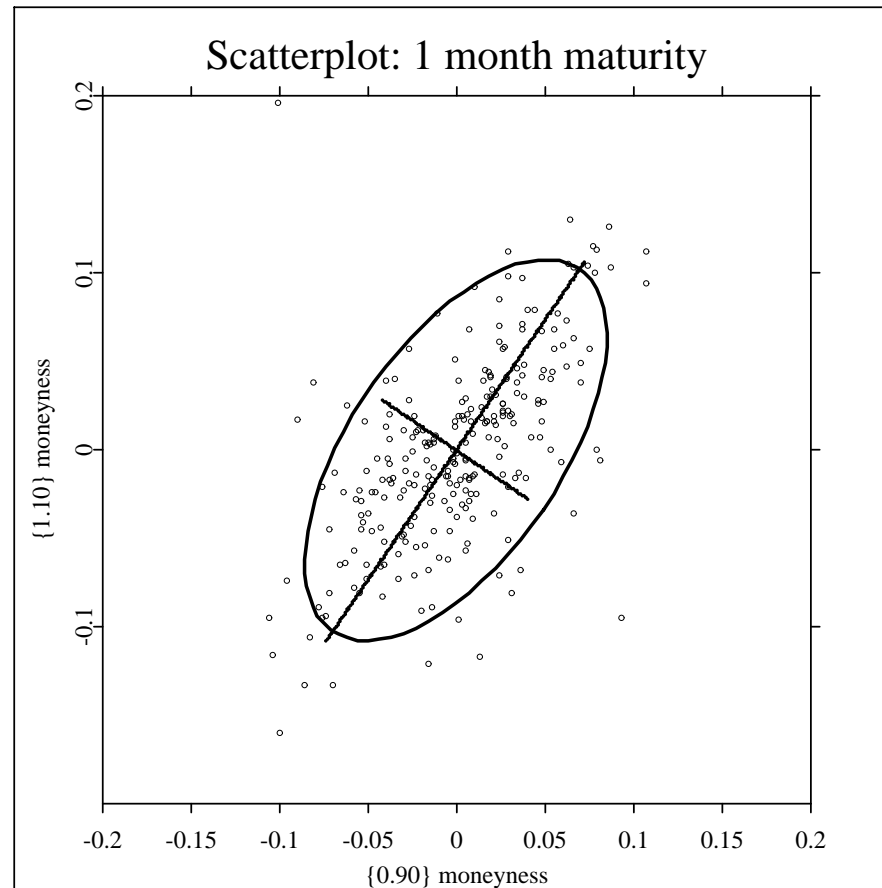
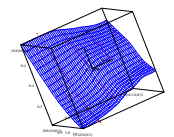


Figure 12: 1 months maturity - moneyness is  $\kappa = 0.90$  against  $\kappa = 1.10$ , ODAX

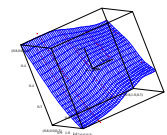


## Solution of this dimension reduction problem:

The spectral decomposition of the covariance matrix  $\Psi$ , i.e.

$$\Psi = \Gamma \Lambda \Gamma^\top$$

- $\Gamma = (\gamma_1 : \gamma_2 : \dots : \gamma_p)$  the matrix of **eigenvectors**. Eigenvectors are **principle axes** of the hyper-ellipsoid.
- $\Lambda = \text{diag}(\lambda_1, \lambda_2, \dots, \lambda_p)$  are the **eigenvalues**. Eigenvalues are the **variances** of principal components.
- $Y = \Gamma^\top X$  are the **principal components**.



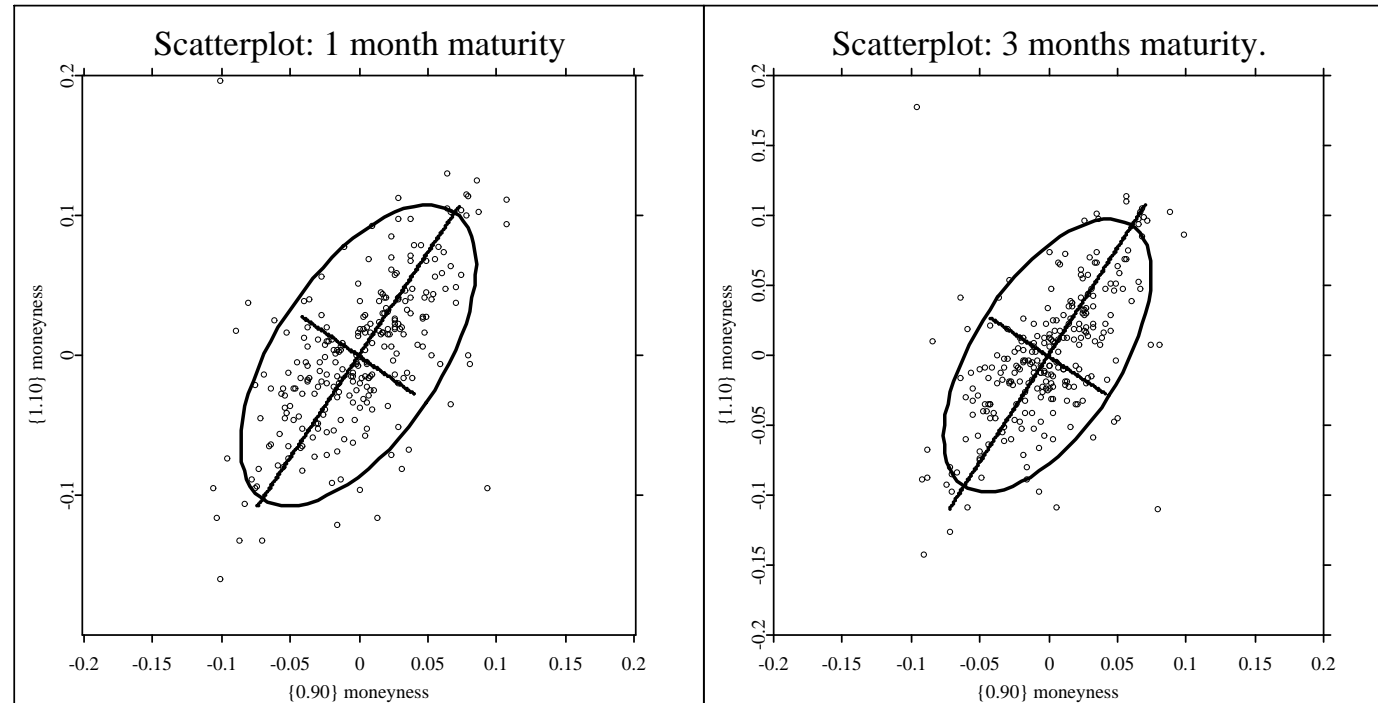
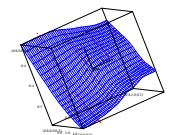


Figure 13: 1 and 3 months maturity - moneyness is  $\kappa = 0.90$  against  $\kappa = 1.10$ , separate PCA; ODAX

 [CPCpca.xpl](#)



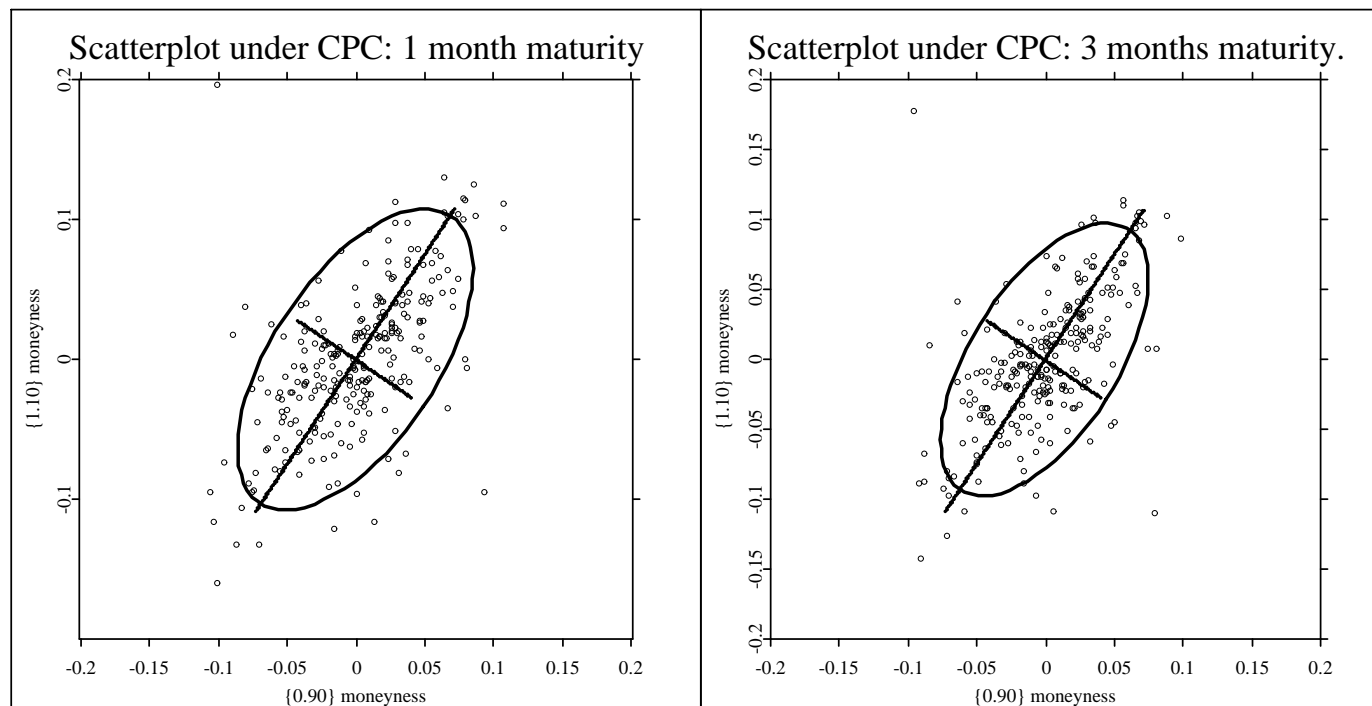
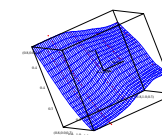


Figure 14: 1 and 3 months maturity - moneyness is  $\kappa = 0.90$  against  $\kappa = 1.10$ , common PCA, ODAX

 [CPCcpc.xpl](#)



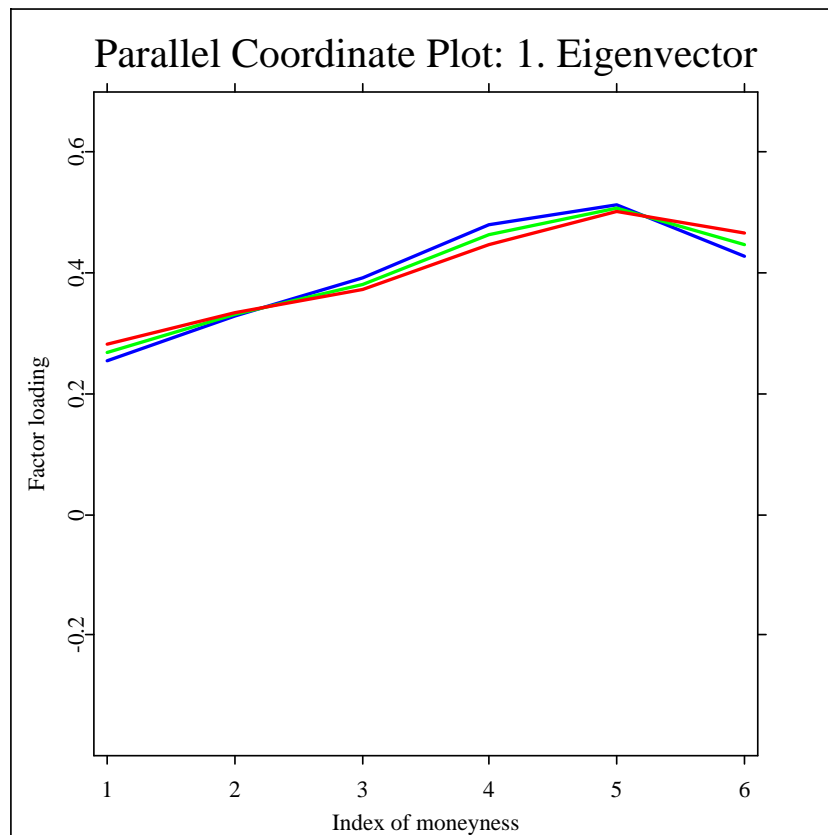
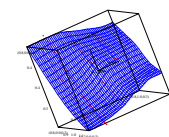


Figure 15: 1<sup>st</sup> eigenvectors (sep. PCA) for 1, 2 and 3 months maturity – index 1 to 6 is  $\kappa \in \{0.85, 0.90, 0.95, 1.00, 1.05, 1.10\}$





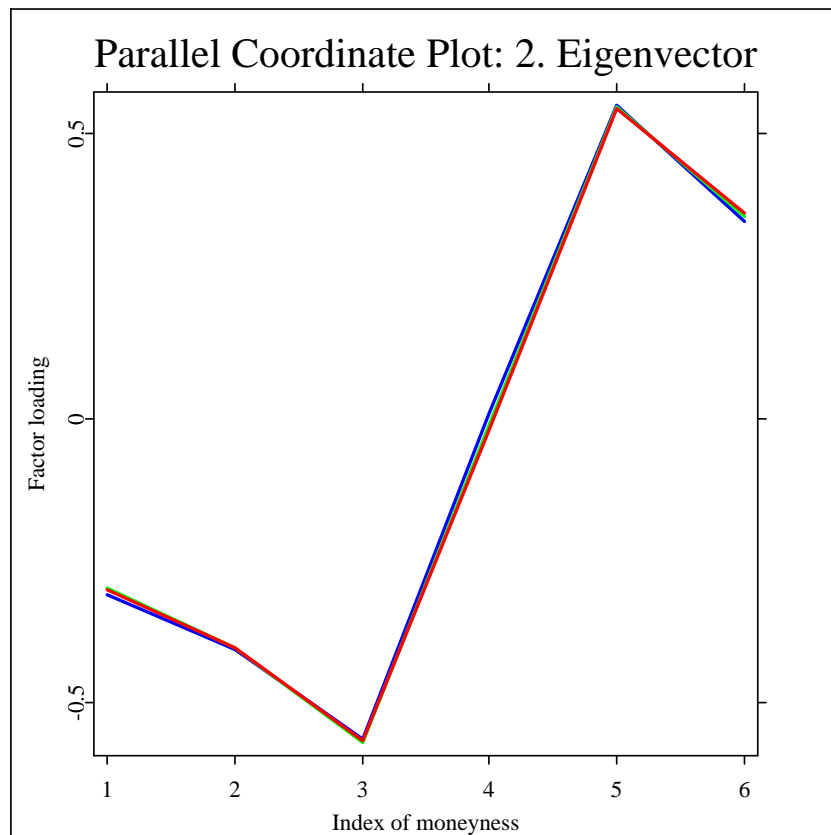
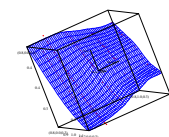


Figure 16:  $2^{nd}$  eigenvectors (sep. PCA) for 1, 2 and 3 months maturity – index 1 to 6 is  $\kappa \in \{0.85, 0.90, 0.95, 1.00, 1.05, 1.10\}$



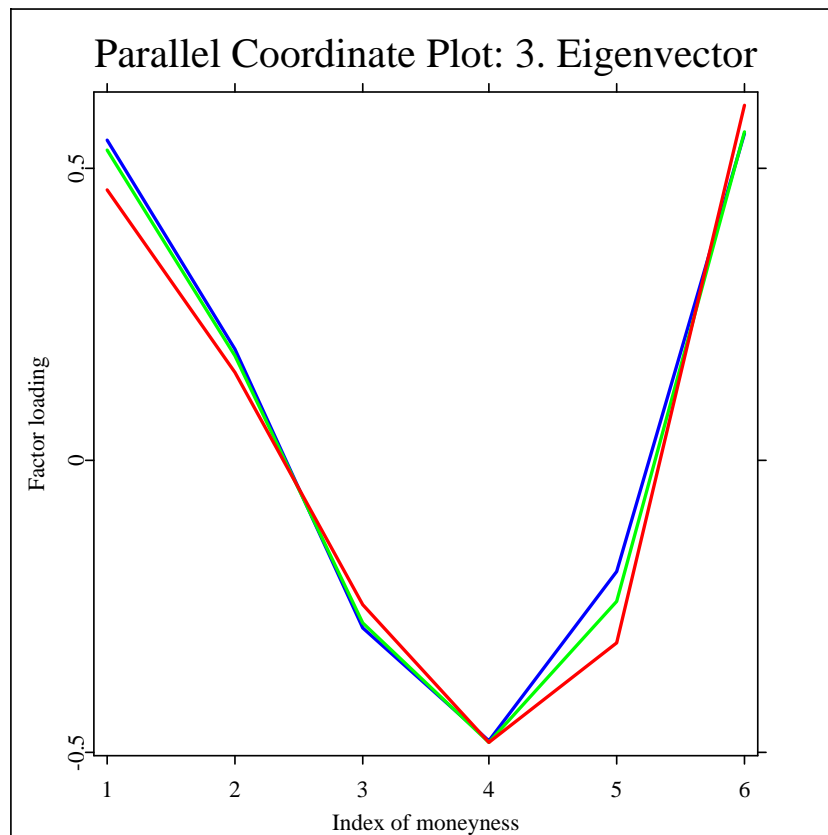
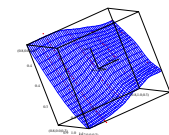


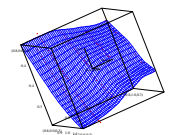
Figure 17: 3<sup>rd</sup> eigenvectors (sep. PCA) for 1, 2 and 3 months maturity – index 1 to 6 is  $\kappa \in \{0.85, 0.90, 0.95, 1.00, 1.05, 1.10\}$



# Common Principle Components

## Essential Idea

- As eigenvectors are quite similar across maturity groups, restrict them to be **equal**.
- As eigenvalues differ between groups, allow them to **vary**.
- Therefore, estimate **principal axes common** to all maturity groups, but allow for **different variability** of **principal components**.



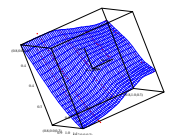
## The CPC-Hypothesis

$$H_{\text{CPC}} : \Psi_i = \Gamma \Lambda_i \Gamma^\top, \quad i = 1, \dots, k. \quad (1)$$

$\Psi_i$  are positive definite  $p \times p$  population covariance matrices,  $\Gamma$  is an orthogonal  $p \times p$  matrix and  $\Lambda_i = \text{diag}(\lambda_{i1}, \dots, \lambda_{ip})$ .

Let  $S_i$  be the (unbiased) sample covariance matrix of implied volatility returns, which are assumed to stem from an underlying  $p$ -variate normal distribution  $N_p(\mu, \Psi_i)$ . Sample size is  $n_i (> p)$ . Then the distribution of  $S_i$  is a generalization of the chi-squared variate, the Wishart distribution (Muirhead, 1982, p.86) with  $n_i - 1$  degrees of freedom, denoted by

$$n_i S_i \sim \mathcal{W}_p(\Psi_i, n_i - 1).$$

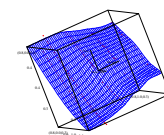


For the  $k$  Wishart matrices  $S_i$  the likelihood function is

$$L(\Psi_1, \dots, \Psi_k) = C \prod_{i=1}^k \exp \left\{ \text{tr} \left( -\frac{1}{2} (n_i - 1) \Psi_i^{-1} S_i \right) \right\} |\Psi_i|^{-\frac{1}{2} (n_i - 1)} \quad (2)$$

where  $C$  is a constant not depending on the parameters. The likelihood function has to be maximized under the orthogonality conditions

$$\gamma_m^\top \gamma_j = \begin{cases} 0 & m \neq j \\ 1 & m = j \end{cases}.$$

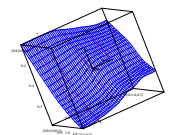


Maximizing the likelihood is equivalent to minimizing the function

$$\begin{aligned}
 g(\Psi_1, \dots, \Psi_k) &= -2 \log L + 2 \log C \\
 &= \sum_{i=1}^k (n_i - 1) \left\{ \ln |\Psi_i| + \text{tr}(\Psi_i^{-1} S_i) \right\}. \quad (3)
 \end{aligned}$$

Assuming that  $H_{\text{CPC}}$  in equation (1) holds, yields

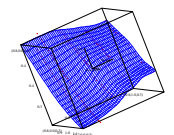
$$g(\Gamma, \Lambda_1, \dots, \Lambda_k) = \sum_{i=1}^k (n_i - 1) \sum_{j=1}^p \left( \ln \lambda_{ij} + \frac{\gamma_j^\top S_i \gamma_j}{\lambda_{ij}} \right). \quad (4)$$



We impose the orthogonality constraints by the Lagrange method, where  $\mu_j$  denotes the Lagrange multiplier of the  $p$  constraints  $\gamma_j^\top \gamma_j = 1$ , and  $\mu_{hj}$  the Lagrange multiplier for the  $p(p-1)/2$  constraints  $\gamma_h^\top \gamma_j = 0$  ( $h \neq j$ ). It follows that the function to be minimized is given by

$$g^*(\Gamma, \Lambda_1, \dots, \Lambda_k) = g(\cdot) - \sum_{j=1}^p \mu_j (\gamma_j^\top \gamma_j - 1) - 2 \sum_{h < j} \mu_{hj} \gamma_h^\top \gamma_j. \quad (5)$$

**ebook** [W. Härdle, L. Simar\(2003\): Applied Multivariate Statistical Analysis](#)



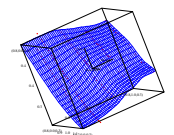
## Solution

By taking partial derivatives w.r.t. all  $\lambda_{im}$  and  $\gamma_m$  and some manipulations, the solution of the CPC model can be written as the generalized system of characteristic equations

$$\gamma_m^\top \left( \sum_{i=1}^k (n_i - 1) \frac{\lambda_{im} - \lambda_{ij}}{\lambda_{im} \lambda_{ij}} S_i \right) \gamma_j = 0, \quad m, j = 1, \dots, p, \quad m \neq j, \quad (6)$$

which needs to be solved using

$$\lambda_{im} = \gamma_m^\top S_i \gamma_m, \quad i = 1, \dots, k, \quad m = 1, \dots, p$$

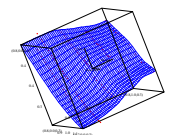




and the constraints

$$\gamma_m^\top \gamma_j = \begin{cases} 0 & m \neq j \\ 1 & m = j \end{cases}.$$

Flury (1988) proves existence and uniqueness of the maximum of the likelihood function, and Flury and Gauthschi (1986) provide a numerical algorithm, which has been implemented in [XploRe](http://www.i-xplore.de/), <http://www.i-xplore.de/>.



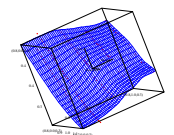
# Partial Common Principle Components

## The partial CPC-Hypothesis

For a partial CPC (pCPC) model of order  $q$ , the hypothesis is given by

$$H_{\text{pCPC}(q)} : \Psi_i = \Gamma^{(i)} \Lambda_i \Gamma^{(i)\top}, \quad i = 1, \dots, k \quad ,$$

where the  $\Psi_i$  are positive definite population covariance matrices, and  $\Lambda_i = \text{diag}(\lambda_{i1}, \dots, \lambda_{ip})$ .  $\Gamma^{(i)} = (\Gamma_c, \Gamma_s^{(i)})$  are orthogonal  $p \times p$  matrices, where  $\Gamma_c$  is  $p \times q$ ,  $q \leq p - 2$  and denotes the matrix of eigenvectors common to all groups, and  $\Gamma_s^{(i)}$  the  $p \times (p - q)$  matrix of eigenvectors that are specific.



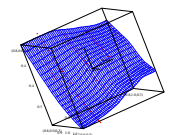
# A Hierarchy of Covariance Matrix Structures

---

Level 1:	Equality	$\Psi_i = \Psi$
Level 2:	Proportionality	$\Psi_i = \rho_i \Psi_1$
Level 3:	CPC	$\Psi_i = \Gamma \Lambda_i \Gamma^\top$
Level 4:	partial CPC(q)	$\Psi_i = \Gamma^{(i)} \Lambda_i \Gamma^{(i)\top}$
Level 5:	Unrelatedness	

---

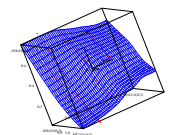
Table 1: Possible hypotheses for all  $i = 1, \dots, k$  groups



# Estimation, Selection, Prediction

## Our Database

- German DAX Options 1999, daily settlement prices, European style
- Calculate implied volatilities by solving the Black Scholes formula for  $\hat{\sigma}$  with observed market prices
- Replace all in-the-money call (put) options by their implicit out-of-the-money put (call)
- Omit prices less than 1/10 Euro, and maturities less than 10 days
- Smooth the implied volatility surface 1999 nonparametrically (stored in MD\*base database containing the volatility surface from 1995-2001, <http://www.mdtech.de> )



# Akaike and Schwarz Information Criteria (AIC, SIC)

The AIC is defined by

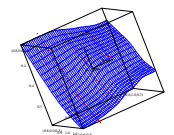
$$\begin{aligned} AIC &= -2 (\text{maximum of log-likelihood}) \\ &+ 2 (\text{number of parameters estimated}). \end{aligned}$$

Assume there are  $I$  hierarchically ordered models, with  $r_1 < r_i < \dots < r_I$  ( $i = 1, \dots, I$ ) parameters in model  $i$ .

Define a modified AIC (Flury, 1988) as

$$AIC(i) = -2(L_i - L_I) + 2(r_i - r_1)$$

where  $L_i$  is the maximum of the log-likelihood function of model  $i$ .



We have

$$AIC(I) = 2(r_I - r_1) \quad \text{and} \quad AIC(1) = -2(L_1 - L_I)$$

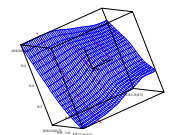
such that

- $AIC(I)$  is twice the difference of the number of parameters of the two extreme models
- $AIC(1)$  is equal to the chi-square test statistic for comparing these two models.

Define a modified SIC as

$$SIC(i) = -2(L_i - L_I) + 2(r_i - r_1) \ln(N),$$

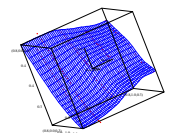
where  $N = \sum_{i=1}^k n_i$  (sum of all observations across  $k$  groups).



## Results: 1, 2, and 3 months maturity

Model		$\chi^2$	df	<i>p</i> -val	AIC	SIC
higher	lower					
Equality	Proport.	237.0	2	0.00	352.0	352.0
Proport	CPC	82.7	10	0.00	118.0	127.7
CPC	pCPC(4)	7.1	2	0.03	55.7	111.3*
pCPC(4)	pCPC(3)	0.2	4	1.00*	52.6*	117.4
pCPC(3)	pCPC(2)	8.1	6	0.23	60.4	143.8
pCPC(2)	pCPC(1)	4.5	8	0.81	64.4	175.2
pCPC(1)	Unrelated	11.9	10	0.29	75.9	223.4
Unrelated					84.0	278.5

 [CPCFluryShort.xpl](#)



CPC Coordinate Plot: First three Eigenvectors

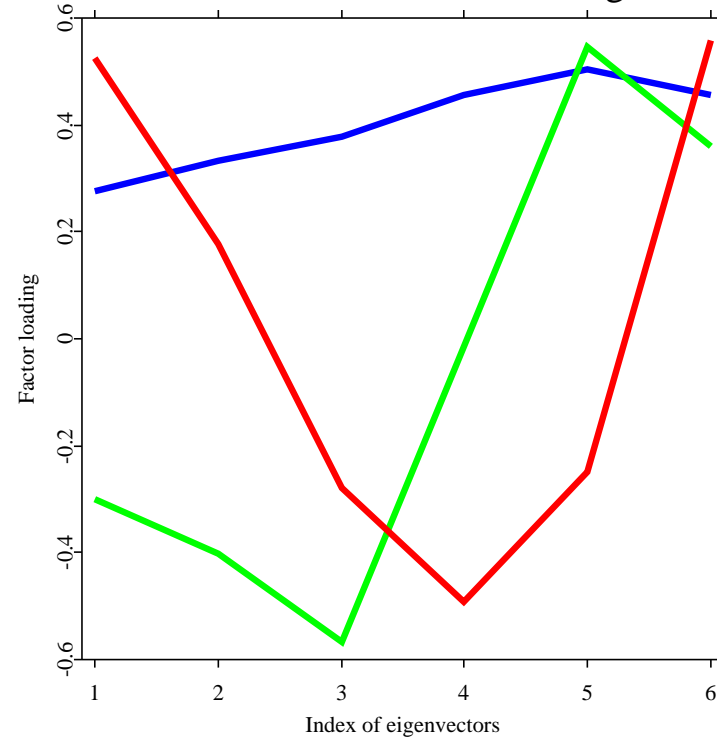
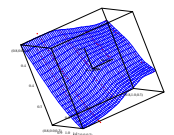


Figure 18: *First three eigenvectors under CPC for 1, 2 and 3 months maturity – index 1 to 6 is  $\kappa \in \{0.85, 0.90, 0.95, 1.00, 1.05, 1.10\}$*

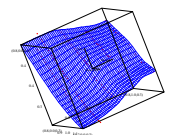
 [CPCpcpCPC.xlsx](#)





# Interpretation of Factor Loadings

- Factor loadings of the **first eigenvector** have the same sign across moneyness and have almost similar size for each moneyness.
- ⇒ Linear combination of volatility returns have almost equal weights across moneyness. Hence, the biggest source of shocks are **up** and **down shocks** of volatility returns (**Shift-Interpretation**).



Volatility Surface: 1st Factor Shock

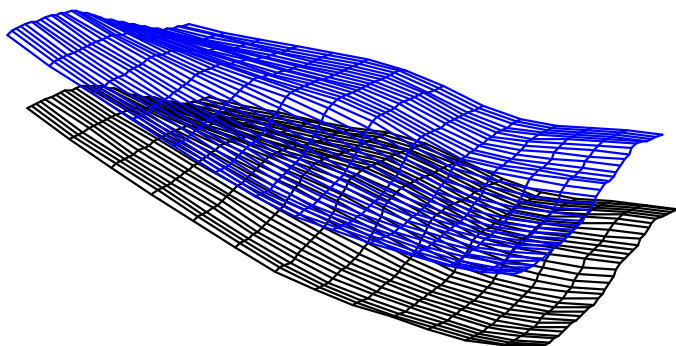
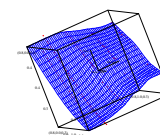
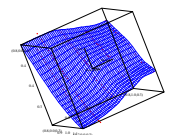


Figure 19: *Simulated Shift Shock: black original, blue after shift shock*



# Interpretation of Factor Loadings

- Factor loadings of the **second eigenvector** have the opposite sign across moneyness, while the weight of ATM options is near to zero.
- ⇒ Volatility returns enter linear combinations with opposite weights at each end of the smile. Therefore, the second biggest source of shocks affects the **slope** of volatility returns (**(Z-)Slope-Interpretation**).



Volatility Surface: 2nd Factor Shock

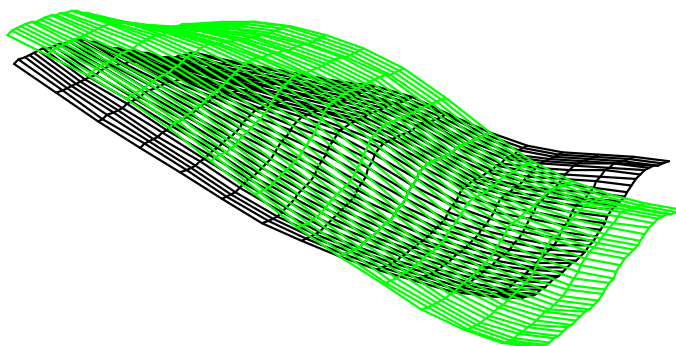
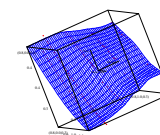
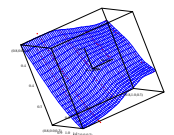


Figure 20: *Simulated Slope Shock: black original, green after slope shock*



# Interpretation of Factor Loadings

- Factor loadings of the **third eigenvector** have the same sign at both ends of the smile and an opposite sign for ATM options.
- ⇒ Volatility returns enter linear combinations with almost the same weights at each end of the smile, and a large opposite one for ATM options. Hence, the third biggest source of shocks affects the **curvature** of volatility returns (**Twist-Interpretation**).



Volatility Surface: 3rd Factor Shock

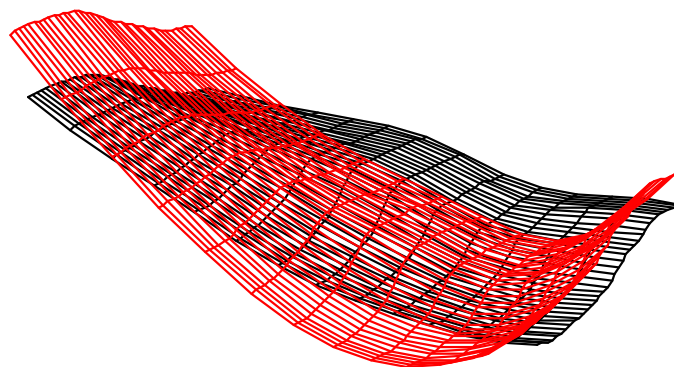
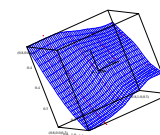


Figure 21: *Simulated Twist Shock: black original, red after twist shock*



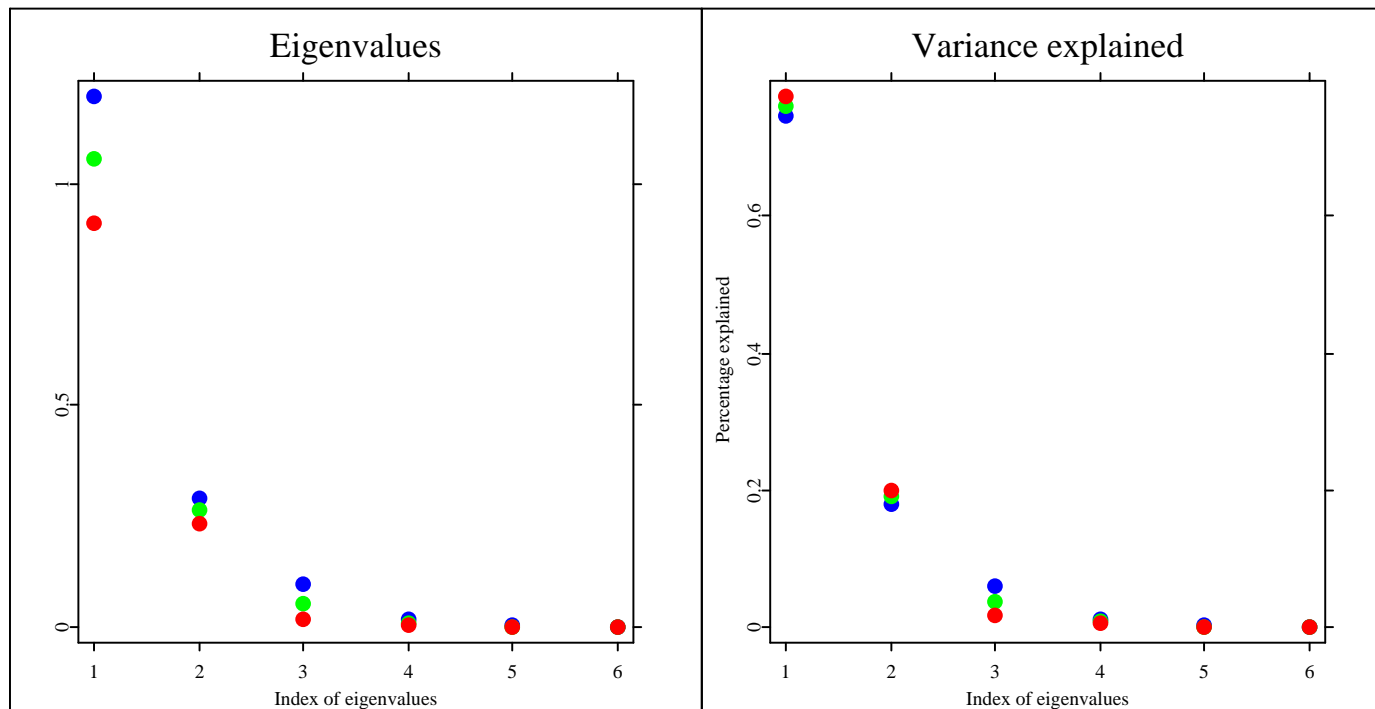
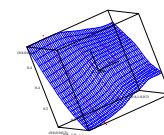


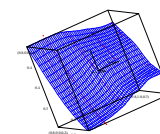
Figure 22: *Eigenvalues and the variance explained as obtained in the CPC model, 1, 2 and 3 months maturity*

 [CPCpcpCPC.xlsx](#)



## Results: 6, 9, 12 months maturity

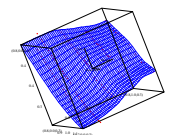
Model		$\chi^2$	df	<i>p</i> -val	AIC	SIC
higher	lower					
Equality	Proport.	250.8	2	0.00	486.0	486.0
Proport	CPC	81.0	10	0.00	239.0	248.5
CPC	pCPC(4)	5.3	2	0.07	178.0	233.8
pCPC(4)	pCPC(3)	4.0	4	0.40	177.0	241.8
pCPC(3)	pCPC(2)	109.5	6	0.00	182.0	264.3
pCPC(2)	pCPC(1)	19.2	8	0.01	89.4	194.6*
pCPC(1)	Unrelated	16.2	10	0.09	83.6*	228.4
Unrelated					84.0	278.5





# Interpretation of Factor Loadings

- Eigenvectors exhibit similar patterns as seen for short maturities, hence interpretation stays the same. Only shift factor is common across groups, while factor loadings for the other shocks may differ.
- Between the same principle components of different groups a scaling property is visible.
- The expiry behavior is mostly captured by the third component: observe the regular spikes in the black line of Figure 58.



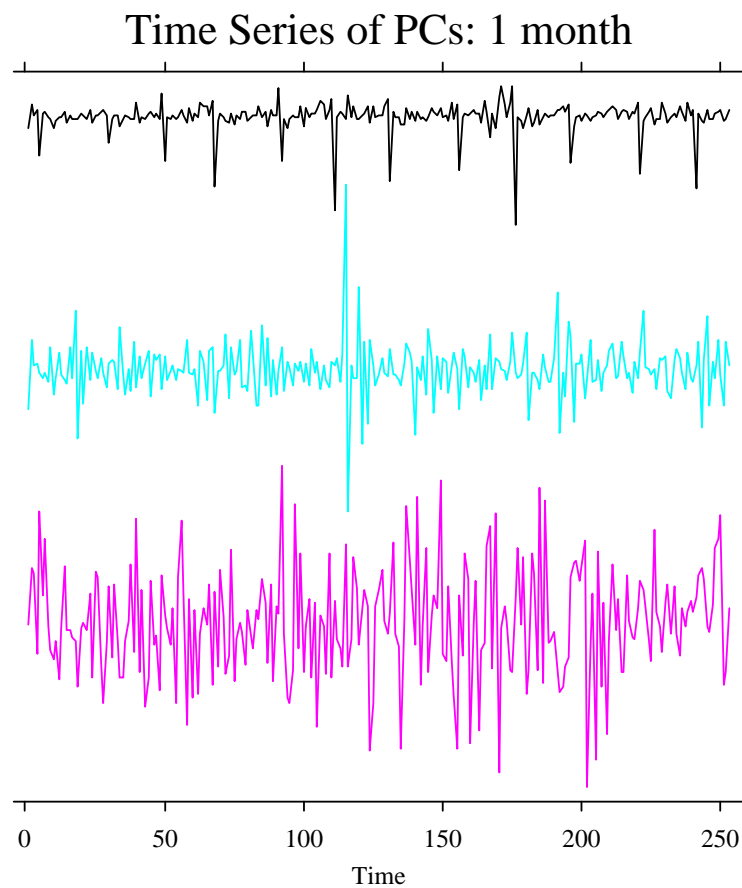
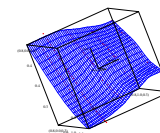


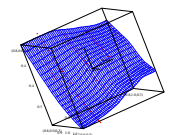
Figure 23: *1st, 2nd and 3rd principal component of the 1 months maturity*



## General Statistics of PCs (3 months)

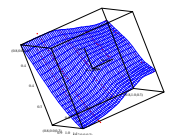
Component	Variance explained	Standard deviation	Skewness	Kurtosis	Correlation with underlying
1	0.88	0.078	0.34	4.12	-0.48
2	0.06	0.020	0.30	6.54	0.08
3	0.03	0.015	0.22	7.30	-0.03

Table 2: *Descriptive statistics of principal components (daily); ODAX.*



## Summary: General Statistics of PCs

- skewness is close to zero for the three PCs
- evidence for excess kurtosis especially in the second and third PC
- evidence for 'leverage effect': correlation with the returns of underlying is around -0.5 for the first component. When there is a negative shock in the market value of the firm, (implied) volatility rises, since the shock results into an increase of the debt-equity ratio
- negligible correlation with underlying in the second the third component



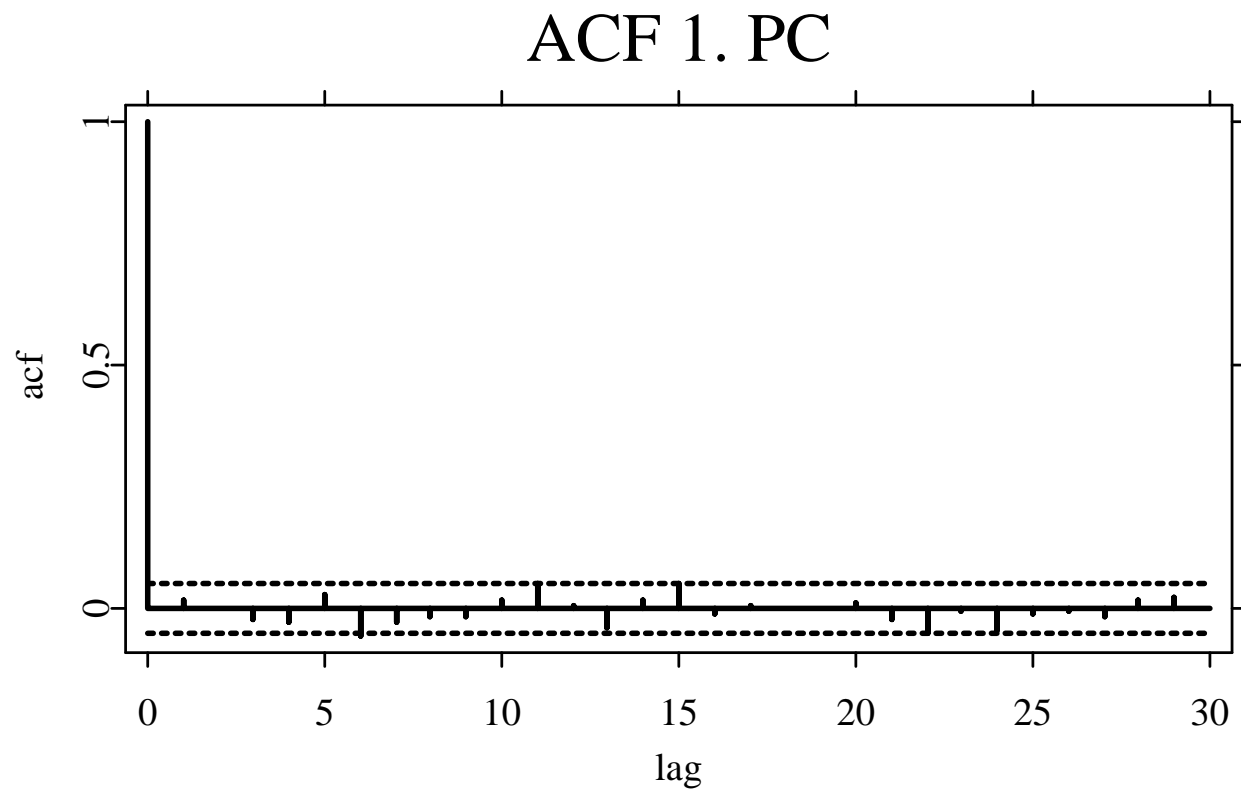
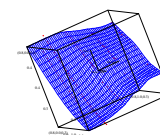


Figure 24: *Autocorrelation function of the 1. PC.*



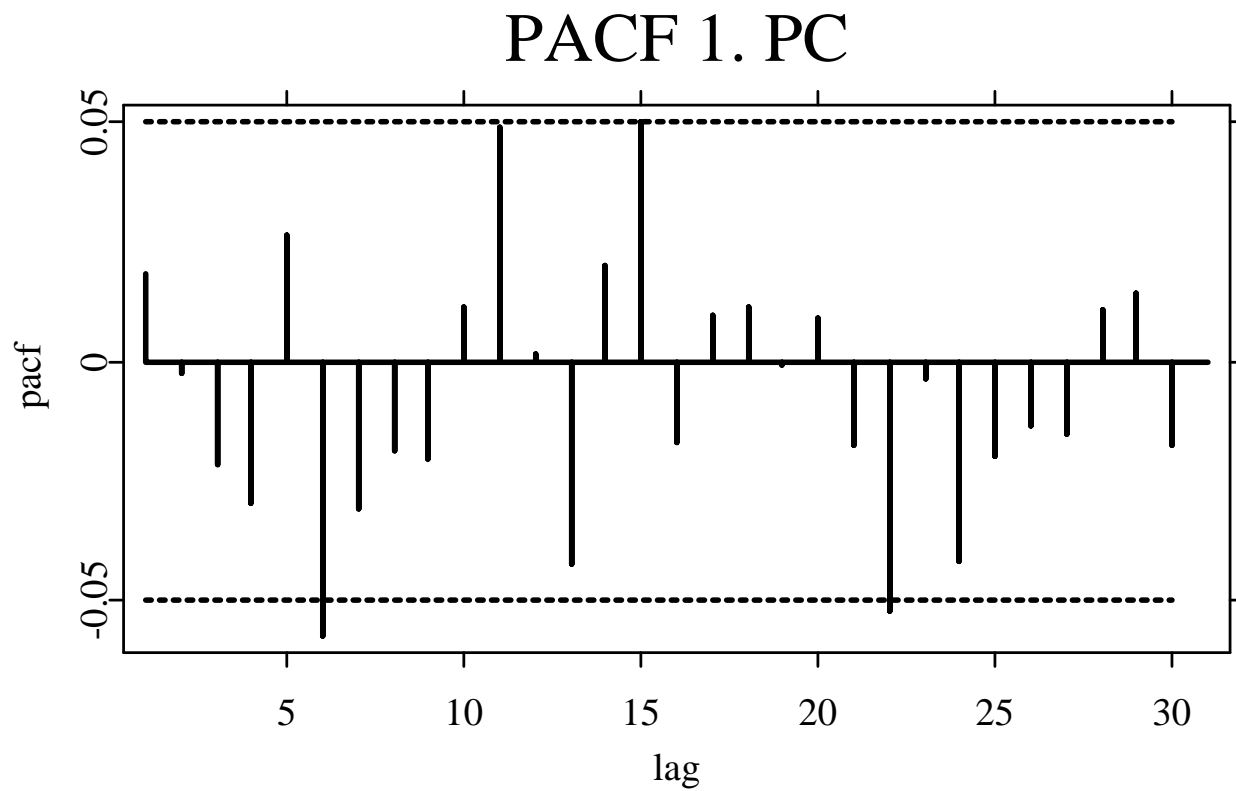
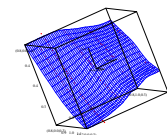


Figure 25: *Partial autocorrelation function of the 1. PC.*



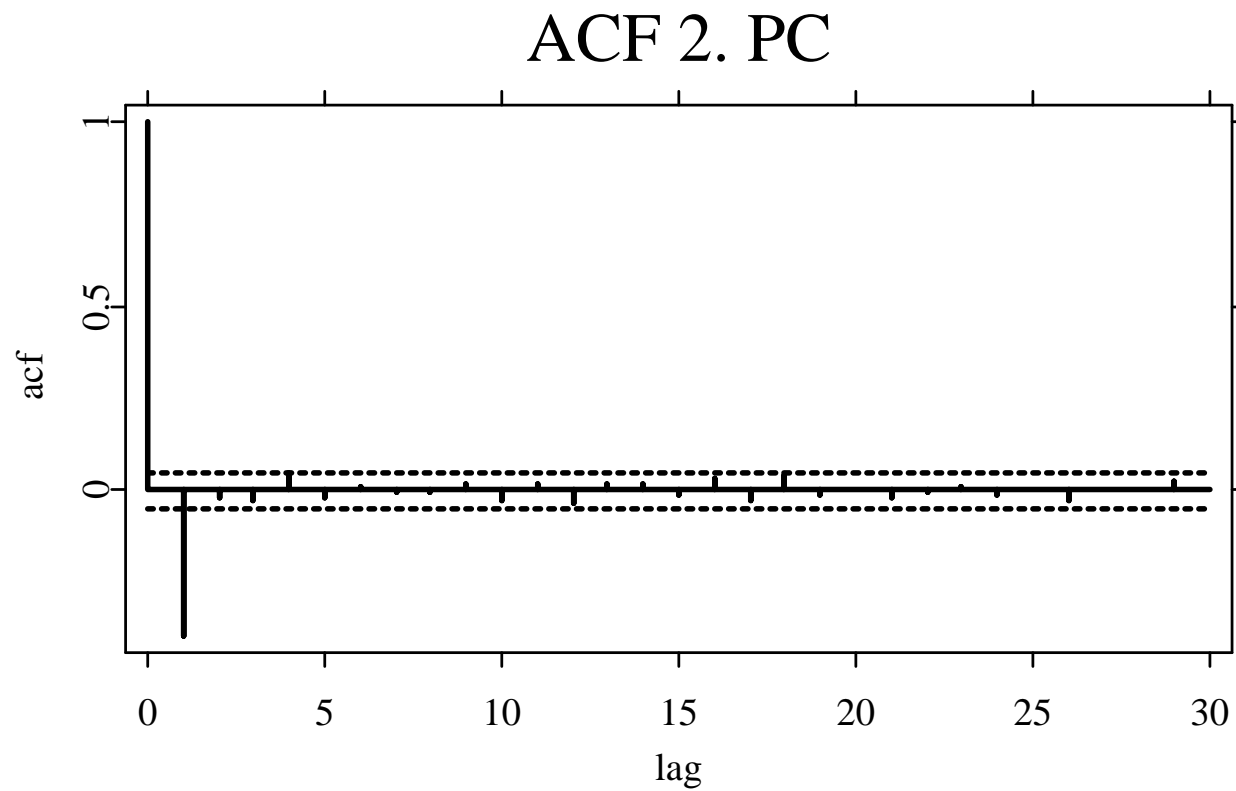
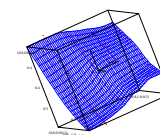


Figure 26: *Autocorrelation function of the 2. PC.*



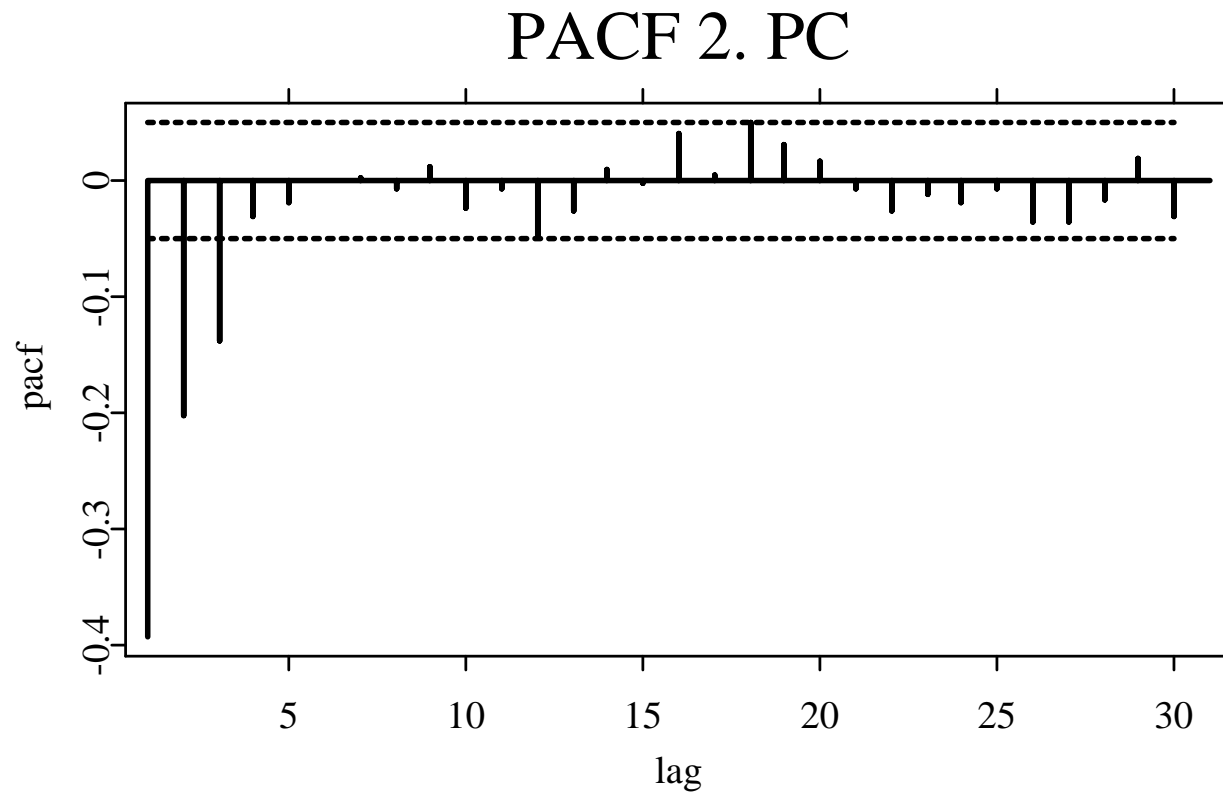
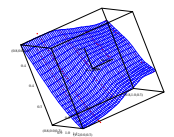


Figure 27: *Partial autocorrelation function of the 2. PC.*





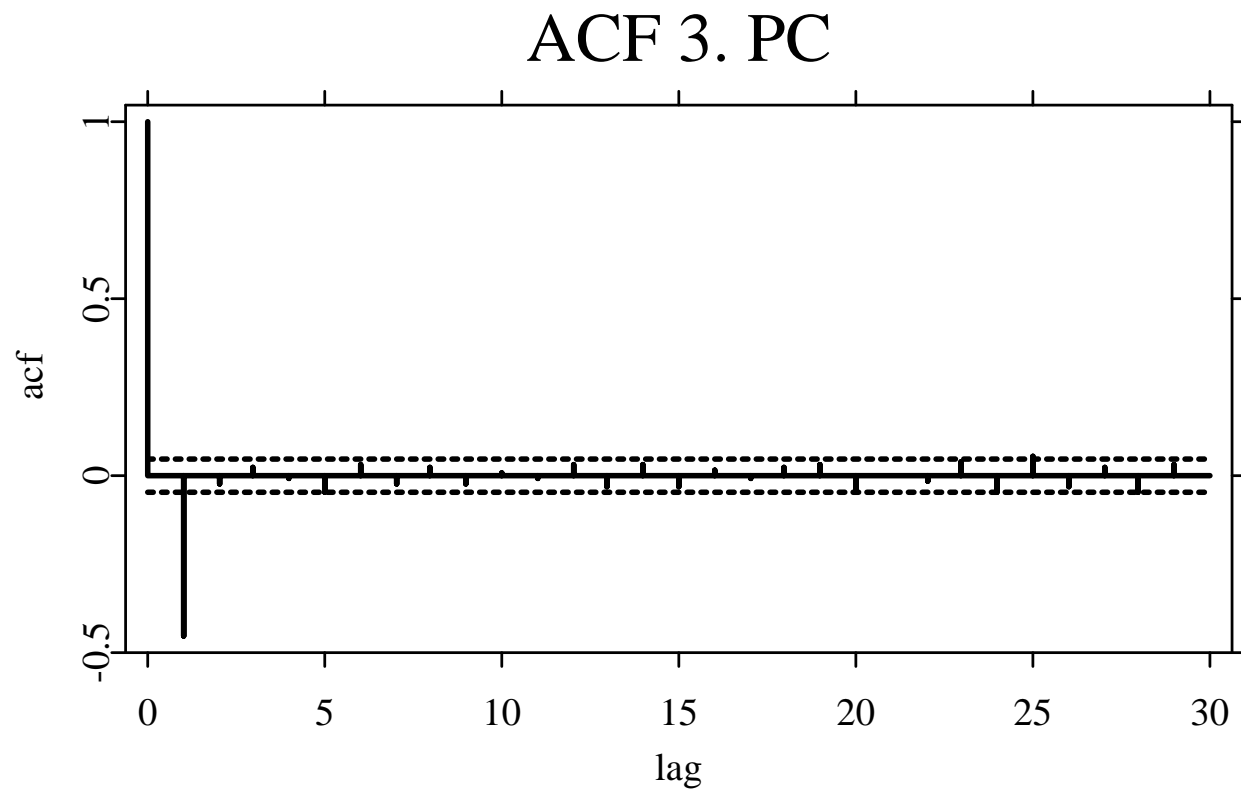
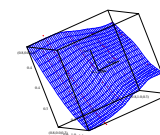


Figure 28: *Autocorrelation function of the 3. PC.*



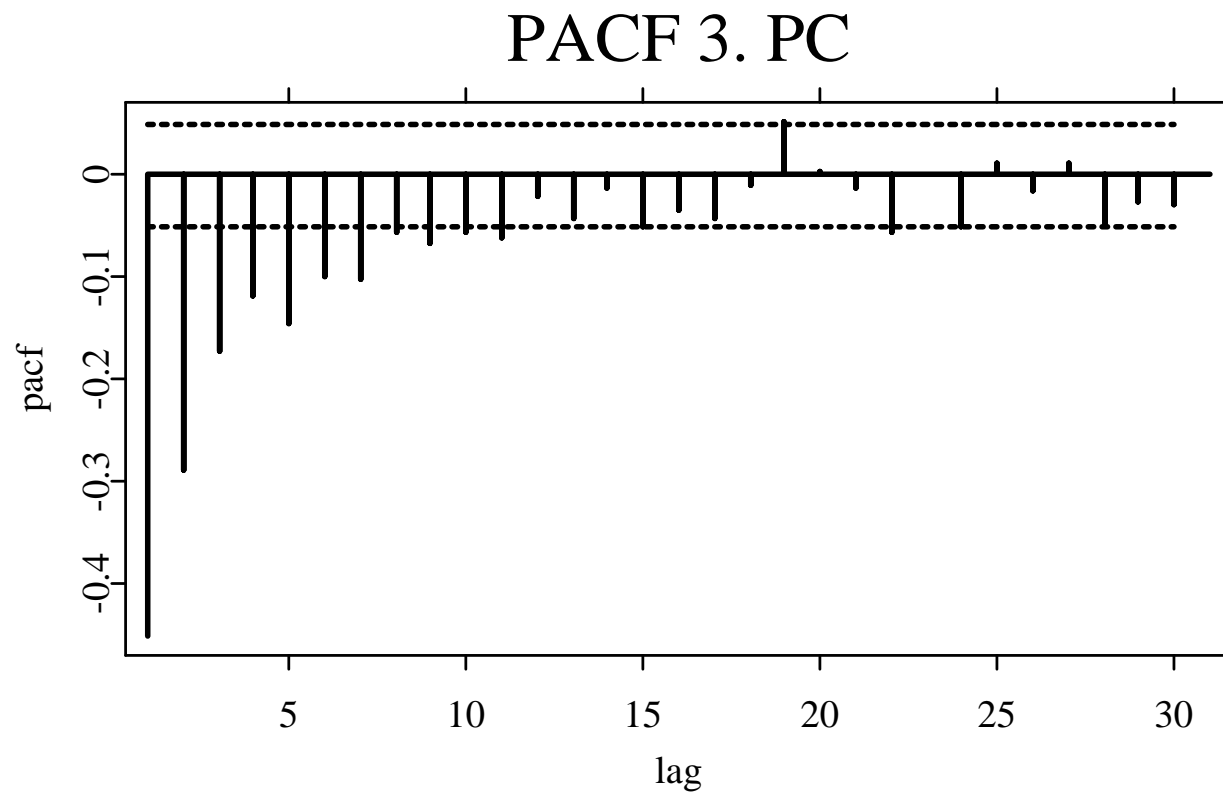
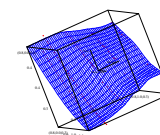


Figure 29: *Partial autocorrelation function of the 3. PC.*



From the autocorrelation and partial autocorrelation function we propose MA( $q$ )-GARCH( $r, s$ ) models:

$q = 0$     $r = 1, 2$     $s = 1, 2$    for  $y_{1t}$  (1. PC), and

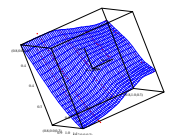
$q = 1$     $r = 1, 2$     $s = 1, 2$    for  $y_{2t}$  (2. PC) and  $y_{3t}$  (3. PC)

$$y_{it} = c + a_1 z_t + \varepsilon_{it} + b_1 \varepsilon_{i,t-1}, \quad (7)$$

$$\varepsilon_{it} \sim \mathcal{N}(0, \sigma_{it}^2),$$

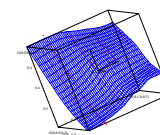
$$\sigma_{it}^2 = \omega + \sum_{j=1}^k \alpha_j \sigma_{i,t-j}^2 + \sum_{j=1}^s \beta_j \varepsilon_{i,t-j}^2 + \gamma z_t^2, \quad (8)$$

where  $z_t$  denotes log returns in the DAX index.



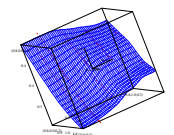
We conduct AIC-SIC searches over a large variety of models:

- For  $y_{1t}$  both AIC and SIC suggest an GARCH(1,2) specification.
- For  $y_{2t}$  and  $y_{3t}$ , a MA(1)-GARCH(1,1) is preferred.



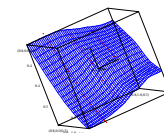
cond. mean	Factor		
	$y_{1t}$	$y_{2t}$	$y_{3t}$
$c$	0.001 (0.407)	$1.9E^{-4}$ (1.170)	$-3.8E^{-05}$ (-0.592)
$a_1$	-2.920 (-24.46)	0.086 (4.860)	0.005 (0.457)
$b_1$		-0.733 (-35.50)	-0.733 (-35.50)

Table 3: *Mean equation: estimation results of GARCH models for the three principal components,  $t$ -statistics in parenthesis.*



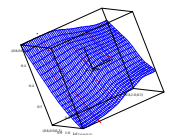
cond. var.	Factor		
	$y_{1t}$	$y_{2t}$	$y_{3t}$
$\omega$	$1.4E^{-4}$ (3.945)	$6.7E^{-5}$ (7.515)	$1.7E^{-05}$ (8.687)
$\alpha_1$	0.803 (32.09)	0.425 (6.774)	0.686 (24.41)
$\beta_1$	0.246 (7.112)	0.200 (6.840)	0.147 (8.027)
$\beta_2$	-0.130 (-4.110)		
$\gamma$	1.480 (4.991)		
$\bar{R}^2$	0.23	0.22	0.33

Table 4: *Variance equation: estimation results of GARCH models for the three principal components, t-statistics in parenthesis.*



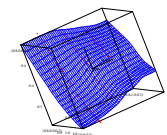
## Summary: Model estimates of 1. PC

- mean equation: index returns have a highly significant impact on 1. PC
- sign of  $a_1$  in line with the 'leverage effect' hypothesis
- variance equation:  $\beta_2 < 0$  may be interpreted as an 'over-reaction correction' in terms of variance: High two-period lagged returns have a dampening impact on variance
- volatility increases also when volatility in the underlying is high ( $\gamma > 0$ )
- adjusted  $\bar{R}^2$  around 23% – however: this is due to index returns: leaving  $z_t$  out of the mean equations reduces  $\bar{R}^2$  to around 0.2%, only



## Summary: Model estimates of 2. and 3. PC

- mean equations of  $y_{2t}$  and  $y_{3t}$ : MA(1) components are negative and significant
- index returns are only significant for  $y_{2t}$  and positively influence the slope structure in the surface.
- positive shocks in the underlying reduce implied volatility levels, while at the same time the slope of the surface is intensified





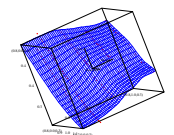
# Checking for model robustness

Model robustness is essential for trading strategies or risk computations.

Two directions of robustness analysis:

1. Choice of data: Settlement prices may be artificially quoted by the exchange. Do we only recover the model of the EUREX?
2. Choice of time period: Is CPC a particular feature of the year 1999?

Perform a CPC analysis for data from 1995 to May 2001 separately in each year, using tick data (= contract data) of puts, calls, and futures observed on the EUREX.



Common Coordinate Plot: First three Eigenvectors

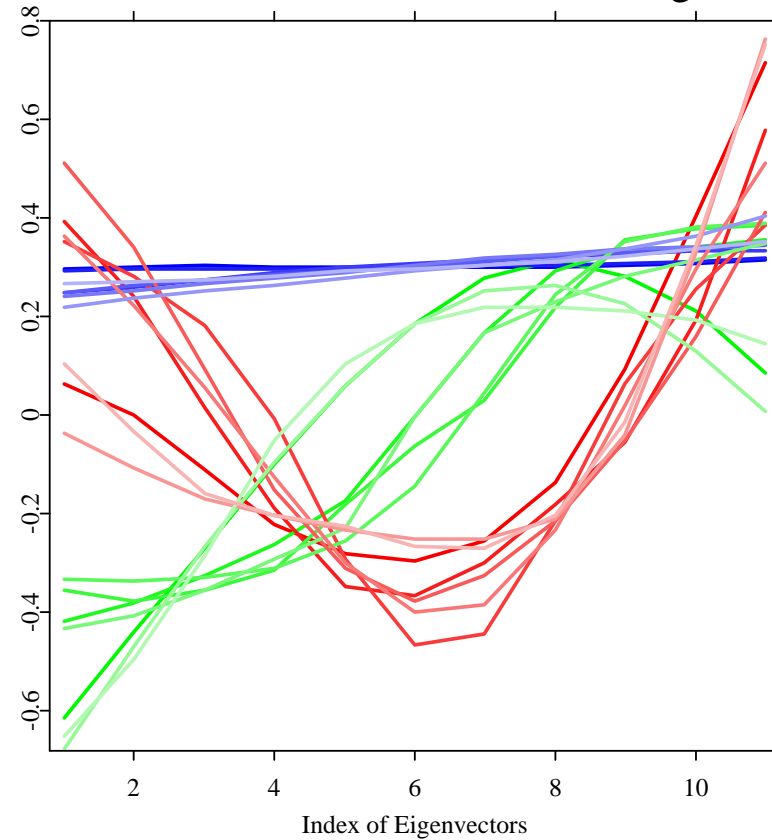
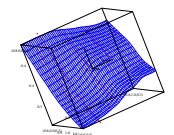


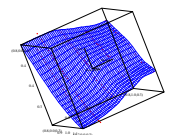
Figure 30: *First, second, and third CPC eigenvectors through the years 1995 to May 2001; increasing color intensity with more recent data, ODAX, EUREX.*



## Results on robustness:

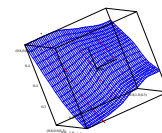
- CPC holds in each year from 1995 to 2001,
- settlement data inherits tick data characteristics,
- shift, slope and twist interpretations remain valid,
- shift component is subject to little time variability,
- slope and twist factors changes slowly over time, and not completely in a non-systematic manner,
- time to maturity component is still captured in the third component.

Tests of time homogeneity of eigenvectors across different sub-samples indicate that it can be necessary to re-estimate the model regularly.



## Volas: What did we learn?

- **CPC** is the preferred modeling strategy for implied volatility returns
- Factor loadings have a natural interpretation (**shift, slope, twist**)
- CPC yields the desired **dimension reduction** of the implied volatility surface



# Trading Strategies, Risk Management

## Values: CPC and State Price Density Dynamics

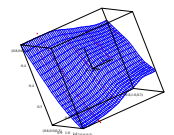
To find the price  $H_t$  of an option take the discounted expected value of the pay-off function with respect to a risk-neutral pricing measure

$f^*(S_T, S_t, \tau)$ :

$$H_t = e^{-r\tau} \mathbb{E}[\psi(S_T, K, \tau) | \mathcal{F}_t] = e^{-r\tau} \int_0^\infty \psi(S_T, K, \tau) f^* dS_T ,$$

where  $\psi$  is the payoff function, e.g.  $\psi = \max(S_T - K, 0)$  in case of the call.

$f^*(S_T, S_t, \tau)$  is also called (implied) State Price Density (SPD).

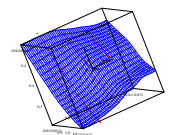


$f^*(S_T, S_t, \tau)$  can be obtained by taking the second derivative of the option price function  $H(S_t, K, r, \tau)$  w.r.t.  $K$ :

$$f^*(S_T, S_t, \tau) = e^{r\tau} \frac{\partial^2 H_t}{\partial K^2} \Big|_{K=S_T},$$

when time to maturity  $\tau$ , the current underlying asset price  $S_t = S$  are fixed, Breeden and Litzenberger (1987).

This derivative can be expressed in terms of moneyness  $M = S/K$  and first and second derivative of the implied volatility surface  $\sigma(M)$ ,  $\sigma'(M)$ ,  $\sigma''(M)$  only, Rookley (1997).



Adopt the following procedure:

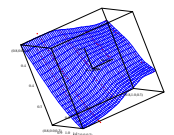
1. Set up a  $q < p$  factor model for the smile at maturity  $\tau_i$

$$\hat{\sigma}_t(\kappa, \tau_i) = \hat{\sigma}_0(\kappa, \tau_i) + \sum_{j=1}^q y_{it} \gamma_j^\top,$$

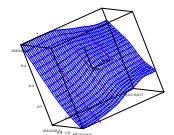
where PCs are modeled as a function in lagged values and exogeneous variables  $Z$  as  $y_{it} = F(y_{t-1}, y_{t-2}, \dots; Z)$ , e.g.

$$\Delta y_{it} = \beta(\bar{y}_i - y_{it-1}) + \varepsilon_t,$$

where  $\bar{y}$  is a long run mean.



2. Other maturity groups are obtained by an appropriate scaling factor  $c(\tau_i)$
3. From the smile estimate  $\sigma'(M)$ ,  $\sigma''(M)$  by a local polynomial method
4. Obtain  $f^*(S_T, S_t, \tau) = e^{r\tau} \frac{\partial^2 H_t}{\partial K^2} |_{K=S_T}$
5. Generate trading signals.





# An Example of SPD Estimates

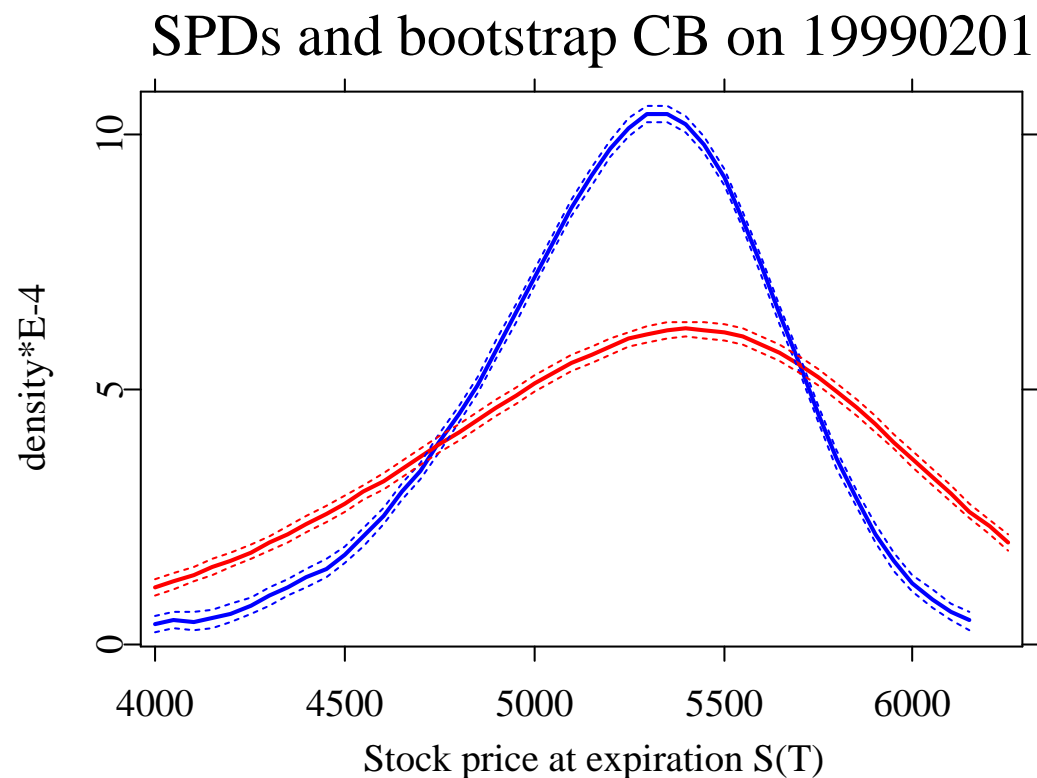
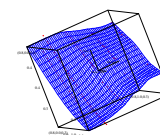
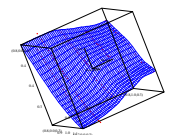


Figure 31: *SPD estimates from ODAX 1999 data by Rookley's method:  $\tau = 1$  month and  $\tau = 2$  months; solid line: density, dashed lines: bootstrap confidence intervals*



Based on this procedure certain trading strategies in options are possible, e.g. skewness and kurtosis trades Aït-Sahalia et al. (2001), Blaskowitz (2001), Härdle and Zheng (2001). They are based on the following idea:

From option data we can extract an **implied** SPD  $f^*$ , based on a cross section of options. However, there is also the **historical** SPD  $g^*$  given by underlying asset's time series data.



## Estimation of historical SPD

Suppose  $S_t$  follows the diffusion process

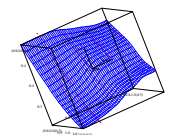
$$dS_t = \mu(S_t)dt + \sigma(S_t)dW_t$$

Consider now the conditional density  $g^*$  generated by the dynamics

$$dS_t^* = (r_{t,\tau} - \delta_{t,\tau})S_t^*dt + \sigma(S_t^*)dW_t^* .$$

The transformation from  $W_t$  to  $W_t^*$ , and  $S_t$  to  $S_t^*$  is an application of Girsanov's Theorem.  $W^*$  is a Brownian Motion under the risk neutral measure,  $r$  the interest rate and  $\delta$  the dividend yield.

Idea: Compare  $g^*$  and  $f^*$ .



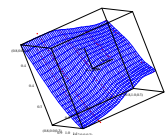
## Estimation of the diffusion function

Florens–Zmirou's (1993) nonparametric estimator for  $\sigma$  (time scale is  $[0,1]$  for expository convenience):

$$\hat{\sigma}_{FZ}(S) = \frac{\sum_{i=1}^{N^*-1} K_{FZ}\left(\frac{S_i - S}{h_{FZ}}\right) N^* \{S_{(i+1)/N^*} - S_{i/N^*}\}^2}{\sum_{i=1}^{N^*} K_{FZ}\left(\frac{S_i - S}{h_{FZ}}\right)},$$

where  $K_{FZ}$  is a kernel function,  $h_{FZ}$  a bandwidth parameter, and  $N^*$  the number of observed index values.

$\hat{\sigma}_{FZ}$  is an unbiased estimator of  $\sigma$  and does not impose any restrictions on the drift.

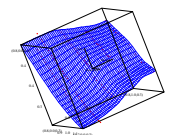


## Computation of historical SPD $g^*$

We use a Monte–Carlo simulation with a Milstein scheme given by

$$S_i = S_{i-1} + rS_{i-1}\Delta t + \sigma(S_{i-1})\Delta W_i + \frac{1}{2}\sigma(S_{i-1})\frac{\partial\sigma}{\partial S}(S_{i-1})\{(\Delta W_{i-1})^2 - \Delta t\},$$

where  $\Delta W_i$  is the increment of a Wiener Process,  $\Delta t$  time between two grid points. The drift is set to  $r$  and  $\frac{\partial\sigma}{\partial S}$  is approximated by  $\frac{\Delta\sigma}{\Delta S}$ .



SPD  $g^*$  may be now obtained by means of a nonparametric kernel density estimation

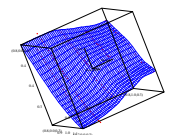
$$g^*(S) = \frac{\hat{p}_t^* \{\log(S/S_t)\}}{S}$$

where

$$\hat{p}_t^*(u) = \frac{1}{Mh} \sum_{m=1}^M K\left(\frac{u_m - u}{h}\right),$$

$u = \log(S/S_t)$  returns and  $M$  is the number of simulated Monte Carlo paths.

$g^*$  is  $\sqrt{N^*}$ -consistent.



Suppose one knew  $f^*$  and  $g^*$ . Are there profitable trading strategies to exploit differences in  $f^*$  and  $g^*$ ? Consider the following situation:

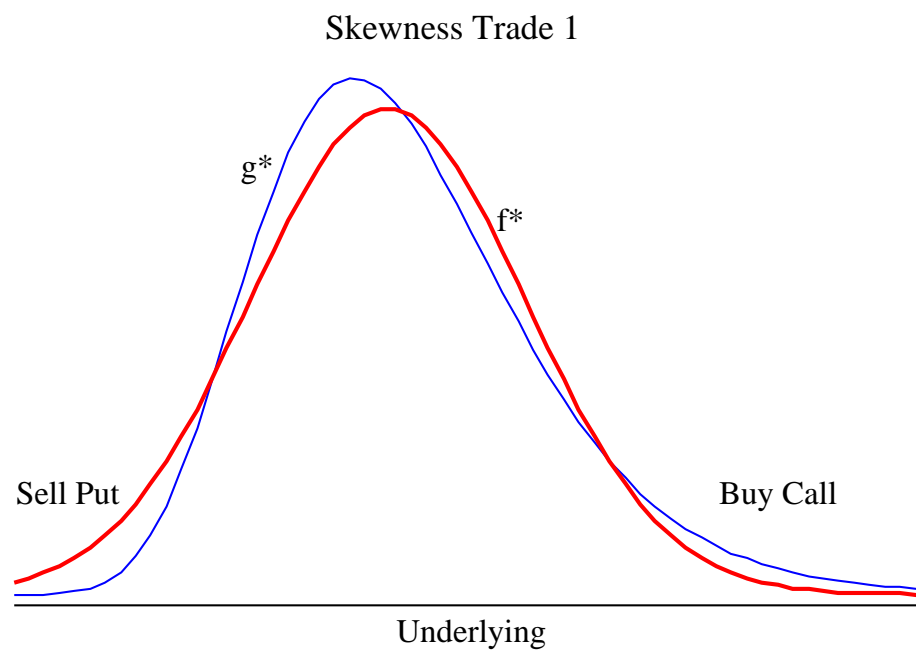
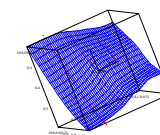
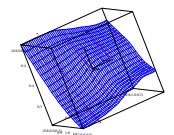


Figure 32: *Skewness trade*



This may be exploited by the following strategies:

Skewness Trade 1	Skewness Trade 2
$\text{skew}(f^*) < \text{skew}(g^*)$	$\text{skew}(f^*) > \text{skew}(g^*)$
Sell OTM Puts	Buy OTM Puts
Buy OTM Calls	Sell OTM Calls

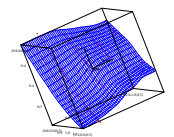




Similarly, kurtosis trades depending on the discrepancies between the two densities  $f^*$  and  $g^*$  can be developed.

Historical simulations show that positive net cash flows may be generated by these kinds of strategies, Aït-Sahalia et al. (2001), Blaskowitz (2001).

However, risk adjusted performance measurement needs to be done and a fine tuning of trading signals remains to be developed.

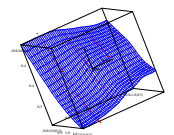


## Values: CPC and Maximum Loss Analysis

The parsimony of the CPC model may also be exploited in the context of Maximum Loss analysis of vega-sensitive, delta-gamma-neutral portfolios (e.g. Fenger, Härdle, Schmidt, 2002).

Consider a Taylor series expansion of a portfolio  $P_t$  built out of  $N$  options:

$$\begin{aligned} \Delta P_t \approx & \sum_{i=1}^N \left( \frac{\partial H_{it}}{\partial \sigma_{it}} \Delta \sigma_{it}(\kappa, \tau) \right. \\ & \left. + \frac{\partial H_{it}}{\partial t} \Delta t + \frac{\partial H_{it}}{\partial r_t} \Delta r_t + \frac{\partial H_{it}}{\partial S_t} \Delta S_t + \frac{1}{2} \frac{\partial^2 H_{it}}{\partial S_t^2} (\Delta S_t)^2 \right) \end{aligned}$$

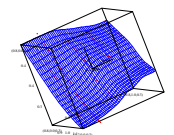


If the portfolio is delta-gamma neutral and if rho and theta-risks can be neglected due to their negligible size, the expression reduces to

$$\Delta P_t \approx \sum_{i=1}^N \frac{\partial H_{it}}{\partial \sigma_{it}} \Delta \sigma_{it}(\kappa, \tau)$$

The CPC model allows us to write the returns of the implied volatilities  $\hat{\sigma}_t(\kappa, \tau)$  as a linear combination of PCs. Thus, taking the respective nearby fixed grid point of the volatility surface  $\hat{\sigma}_t(\kappa_i, \tau_j)$  as a proxy for  $\hat{\sigma}_{it}(\kappa, \tau)$ , one gets:

$$\Delta P_t \approx \sum_{i=1}^N \frac{\partial H_{it}}{\partial \sigma_{it}} \left( \sum_k \gamma_{jk} y_{kt} \right) \hat{\sigma}_{i,t-1}(\kappa, \tau)$$

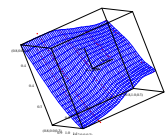


## Definition of Maximum Loss

Maximum loss (ML) is defined as the maximum possible loss

- over a given risk factor space  $A_{\tilde{\tau}}$ , where  $A_{\tilde{\tau}}$  will be assumed a closed set with confidence level  $P(y|y \in A_{\tilde{\tau}}) = \alpha$
- for some holding period  $\tilde{\tau}$ .

In contrast to Value at Risk which requires the profit and loss distribution to be known, ML is directly defined in the risk factor space, Studer (1995).

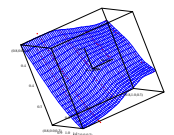


## Constructing $A_{\tilde{\tau}}$

Assuming multi-normally distributed PCs, i.e. the  $y$  obey the joint density function

$$\varphi(y) = \frac{1}{\sqrt{2\pi|\Lambda_i|}} \exp\left(-\frac{1}{2}y^\top \Lambda_i^{-1}y\right),$$

where  $\Lambda_i$  is diagonal matrix of eigenvalues of group  $i$ , construction of the trust region  $A_{\tilde{\tau}}$  is straightforward:



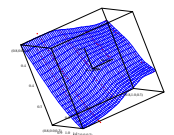
$y^\top \Lambda_i^{-1} y$  is chi-square distributed with  $q$  degrees of freedom, where  $q$  is the number of factors retained for modeling.

Trust region  $A_{\tilde{\tau}}$  is the ellipse given by

$$A_{\tilde{\tau}} = (y | y^\top \Lambda_i^{-1} y \leq c_\alpha),$$

where  $c_\alpha$  denotes the  $\alpha$ -quantile of a chi-squared distribution with  $p$  degrees of freedom.

Fengler, Härdle and Schmidt (2002) consider a simple straddle portfolio over a horizon of one day, where an ATM straddle of short maturities is sold and an ATM straddle of long maturities is bought.



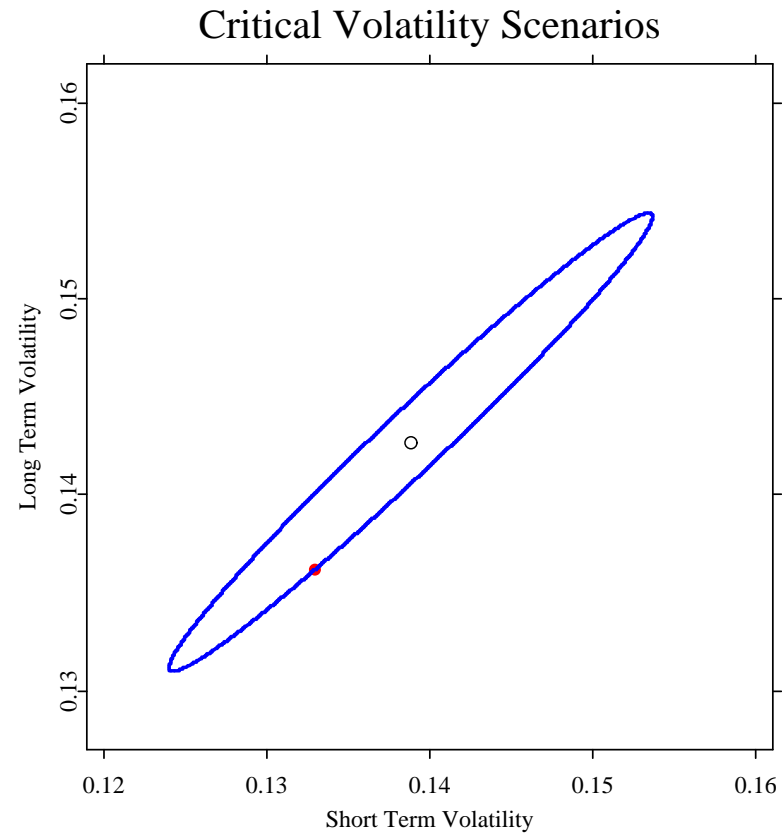
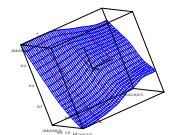


Figure 33: *Critical volatility scenarios for an straddle portfolio on 29/03/96; black circle current level, red circle ML scenario; two factors modeled at  $\alpha = 99\%$ .*



## Changes of Portfolio Values and ML

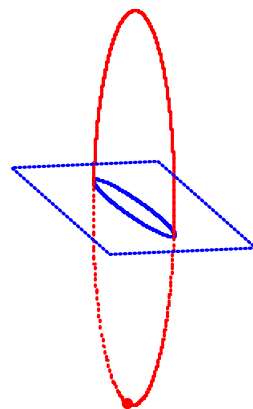
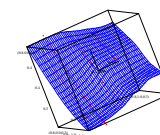


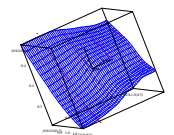
Figure 34: *Critical volatility scenarios for a straddle portfolio on 29/03/96 (blue) portfolio changes (red, gains solid, losses dashed) and ML (red ball); two factors modeled at  $\alpha = 99\%$ .*





Fengler, Härdle and Schmidt (2002) argue that

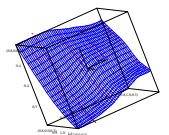
- the procedure can be a convenient guideline tool for daily risk management analysis at trading desks
- the procedure is capable to identify critical volatility scenarios for the portfolio under consideration, even during the Asian crisis 1997
- although the true confidence level of the modelling approach remains unknown, the procedure performs empirically better than is suggested by the number of retained factors
- adaptive methods, notably in the context of *Common Principle Components Analysis* need to be developed to enhance predictability of the the model.



## Volas: What did we learn?

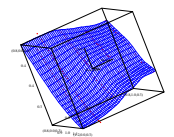
### CPC

- facilitates a high dimensional modeling task by working in a low dimensional manifold,
- factor loadings and common PC factors have natural interpretations in Finance,
- due its generality it is widely applicable in other contexts.



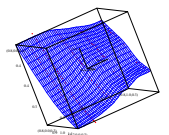
# Voles, Volas, Values: What did we learn?

**Biology and Finance are cross-pollinated by Statistics!**

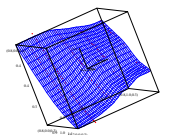


## References

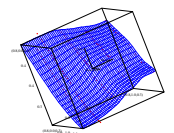
- [1] Airoidi, J.P. and B. Flury (1988) "An application of common principal component analysis to cranial morphometry of *Microtus californicus* and *M. ochrogaster* (Mammalia, Rodentia)." *J. Zool., London* 216, 21-36.
- [2] Aït-Sahalia Y. and A. Lo (1998) "Nonparametric estimation of state-price densities implicit in financial asset prices." *Journal of Finance* 53, 499-548.
- [3] Aït-Sahalia Y. and A. Lo (2000) "Nonparametric risk management and implied risk-aversion." *Journal of Econometrics* 94, 9-51.
- [4] Aït-Sahalia, Wang Y. and Yared, F. (2001), "Do Option Markets correctly Price the Probabilities of Movement of the Underlying Asset?" , *Journal of Econometrics* 102, 67–110.



- [5] Barle, S. and Cakici, N. (1998), "How to Grow a Smiling Tree" *The Journal of Financial Engineering*, 7, 127–146.
- [6] Black F. (1976), "Studies of stock price volatility changes." *Proceedings of the American Statistical Association*, 177-181.
- [7] Blaskowitz, O. (2001), "Trading on Deviations of Implied from Empirical Distributions", Diplomarbeit, Institut für Statistik und Ökonometrie, Humboldt-Universität zu Berlin.
- [8] Breeden and Litzenberger (1987), "Prices of state-contingent claims implicit in option prices." *Journal of Business*, 51, 621–651.
- [9] Derman E. and I. Kani (1997), "Stochastic implied trees: Arbitrage pricing with stochastic term and strike structure of volatility." Quantitative Strategies Technical Notes, Goldman Sachs.
- [10] Dupire, B. (1994), "Pricing with a Smile", *Risk* 7(1), pp. 18-20.

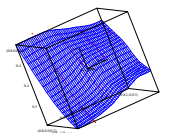


- [11] Fengler, M., Härdle, W. and C. Villa (2001), "The Dynamics of Implied Volatilities: A Common Principle Component Approach", Discussion Paper 38/2001, SFB 373, Humboldt-Universität zu Berlin.
- [12] Fengler, M., Härdle, W. and P. Schmidt (2002), "Common Factors Governing VDAX Movements and the Maximum Loss", forthcoming in: *Journal of Financial Markets and Portfolio Management*.
- [13] Florens-Zmirou, D. (1993), "On Estimating the Diffusion Coefficient from Discrete Observations", *Journal of Applied Probability* 30, pp. 790–804.
- [14] Flury, B. (1988), "Common Principal Components and Related Multivariate Models". Wiley, New York.
- [15] Flury, B. and Gautschi, W. (1986), "An Algorithm for Simultaneous Orthogonal Transformations of Several Positive Definite Matrices to



nearly Diagonal Form", *SIAM Journal on Scientific and Statistical Computing*, 7, 169-184.

- [16] Härdle, W. and J. Zheng (2001), "How Precise are Price Distributions Predicted by Implied Binomial Trees?", mimeo.
- [17] Hull J. and A. White (1987), "The Pricing of Options on Assets with Stochastic Volatilities." *Journal of Finance* 42, 281-300.
- [18] Jarrow R.A. and O'Hara (1989), "Primes and scores: an essay on market imperfections". *Journal of Finance* 44, 1265-1287.
- [19] Rookley, C. (1997), "Fully Exploiting the Information Content of Intra Day Option Quotes: Applications in Option Pricing and Risk Management". University of Arizona, mimeo.
- [20] Rubinstein M. (1985), "Nonparametric tests of alternative option-pricing models using all reported trades and quotes on the 30 most active CBOE option classes from August 23, 1976 through



August 31, 1978." *Journal of Finance* 40, 455-480.

- [21] Schönbucher P.J.(1999), " A Market Model for Stochastic Implied Volatility ", *Working papers*, Department of Statistics, Bonn University.
- [22] Studer, G. (1995), "Value at Risk and Maximum Loss Optimization". RiskLab, Technical Report, Zürich.

Pictures of voles have been taken from

<http://www.nsrl.ttu.edu/tmot1/microchr.htm>

and <http://www.enature.com/>

